Interfaces issues in alternative gate stack structures

Lyudmila Goncharova, Dmitri Starodub, Safak Sayan, David Vanderbilt, Bob Bartynski, Yves Chabal, Torgny Gustafsson and **Eric Garfunkel**

Departments of Chemistry and Physics
Rutgers University, Piscataway, New Jersey 08854 USA
garf@rutchem.rutgers.edu

Collaboration: **Sematech, IBM, Motorola, NIST, Penn State, Intel, TI, IMEC, NCSU, Stanford, Lucent/Agere, UT-Austin…**

Funding: **Sematech, SRC, NSF**

Motivation: Help develop a fundamental understanding nano-electronic interfaces

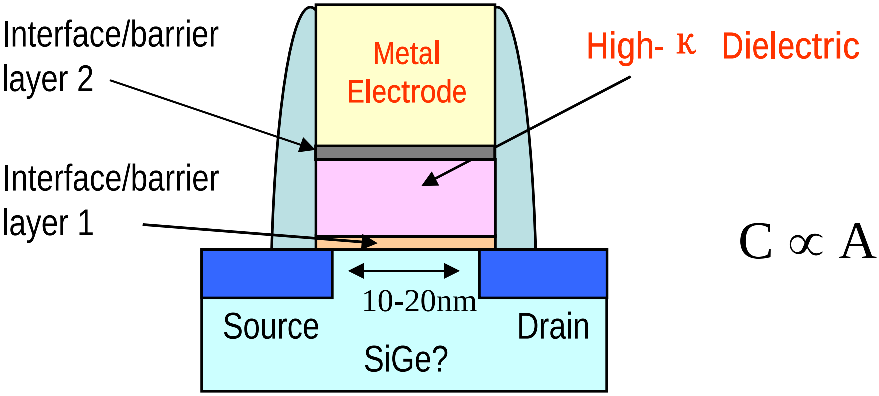

CMOS transistor ~2010?

$C \propto A\varepsilon/d$

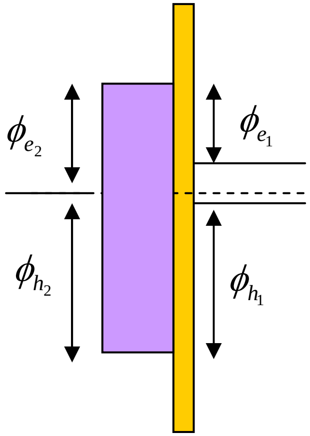

- Interface composition and thermal stability
  - Compositional profiling: medium energy ion scattering (MEIS)
  - Thermal behavior of **high-k films**, interfaces, inter-diffusion….
  - New materials: **metal electrodes**, high-K/GaAs, STO/Si
- Band alignment and electronic structure issues
  - Concepts in “effective work function” engineering: energy diagrams and interface dipoles
  - Experimental tools
  - Examples: high-K dielectrics & metal gate electrodes

Medium energy ion scattering: compositional profiling

MEIS is a high-resolution ion beam based analytical technique:

- mass specific
  - isotope selective
- quantitative
  - total areal density
- sub-nm depth resolution

Rutgers-MEIS uses 100 keV hydrogen projectiles:

- no significant radiation damage during analysis
- straightforward interpretation of scattering spectra

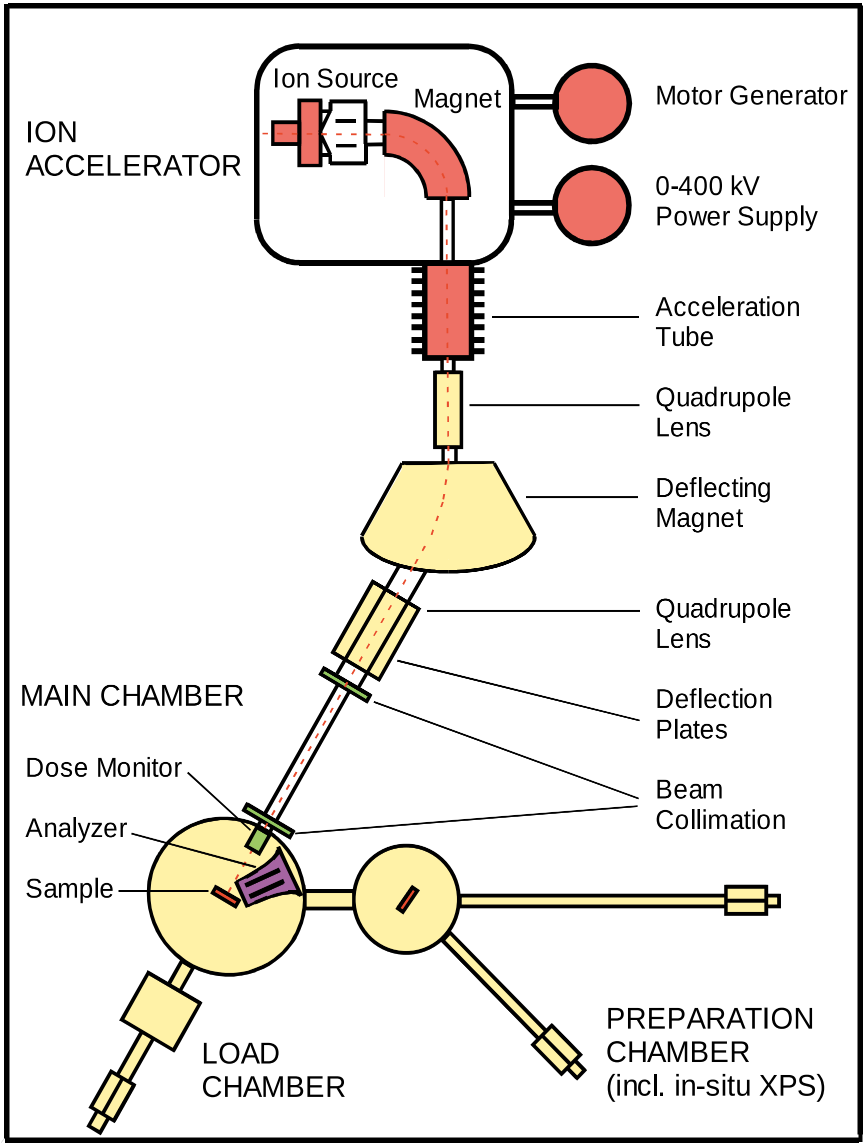

MEIS facility at Rutgers

NRP chamber

beam line

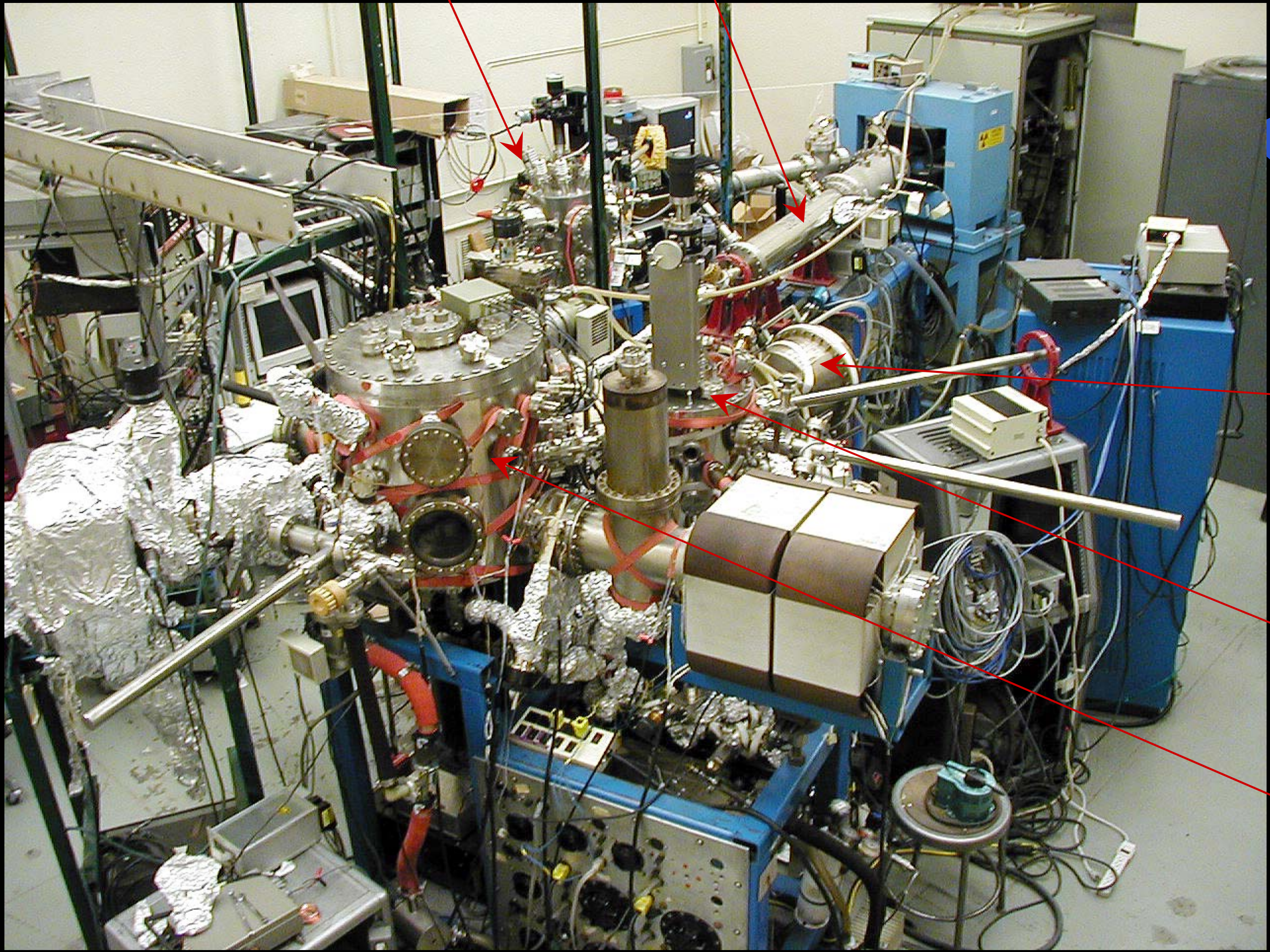

XPS system

preparation chamber

scattering chamber

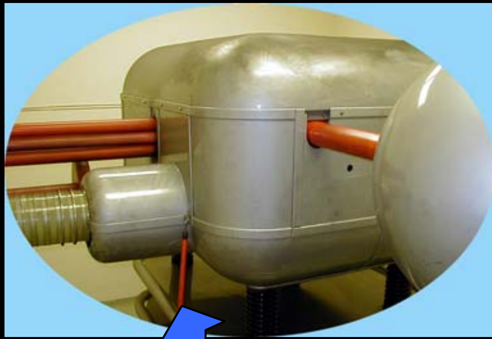

ion implanter

Experimental data

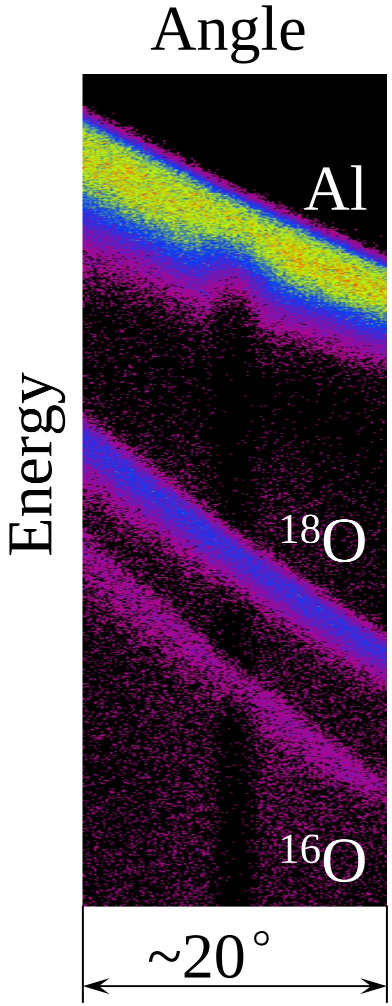

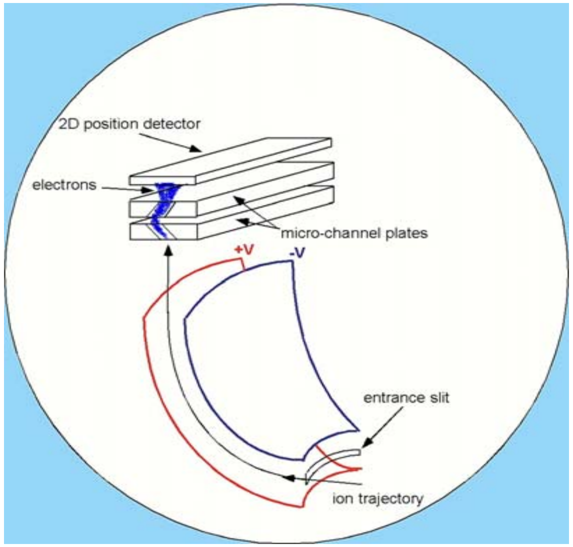

- Energy resolution 140 eV, resulting in depth resolution of ~3 Å near surface
- Angular resolution 0.2°
- Mass-sensitive: $E = E(M, \theta)$
- Quantitative (cross sections are known)

Depth resolution and concentration profiling

Basic concept: Depth profile is based on the energy loss of the ions traveling through the film (stopping power ε ∝ dE/dx ∝ L).

Example: Depth resolution for ≈100 keV protons (resolution of the spectrometer ≈150 eV)

- Stopping power $SiO_2 \approx 12$ eV/Å; $Si_3N_4 \approx 20$ eV/Å; $Ta_2O_5 \approx 18$ eV/Å
- "Near surface" depth resolution ≈ 3-5 Å; worse for deeper layers due to energy straggling

Layer model:

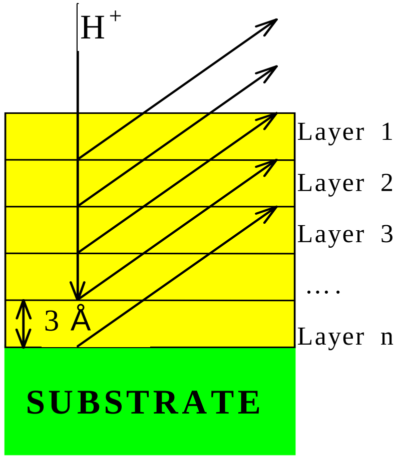

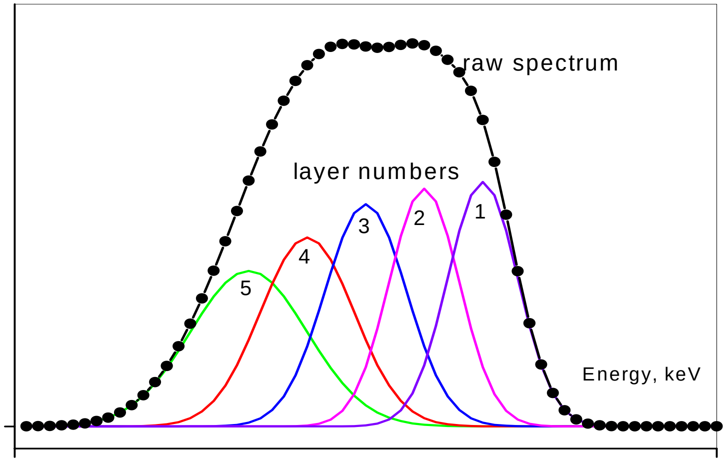

- Areas under each peak corresponds to the concentration of the element in a 3Å slab
- Peak shapes and positions come from energy loss, energy straggling and instrumental resolution.
- The sum of the contributions of the different layers describes the depth profile.

MEIS depth profiling

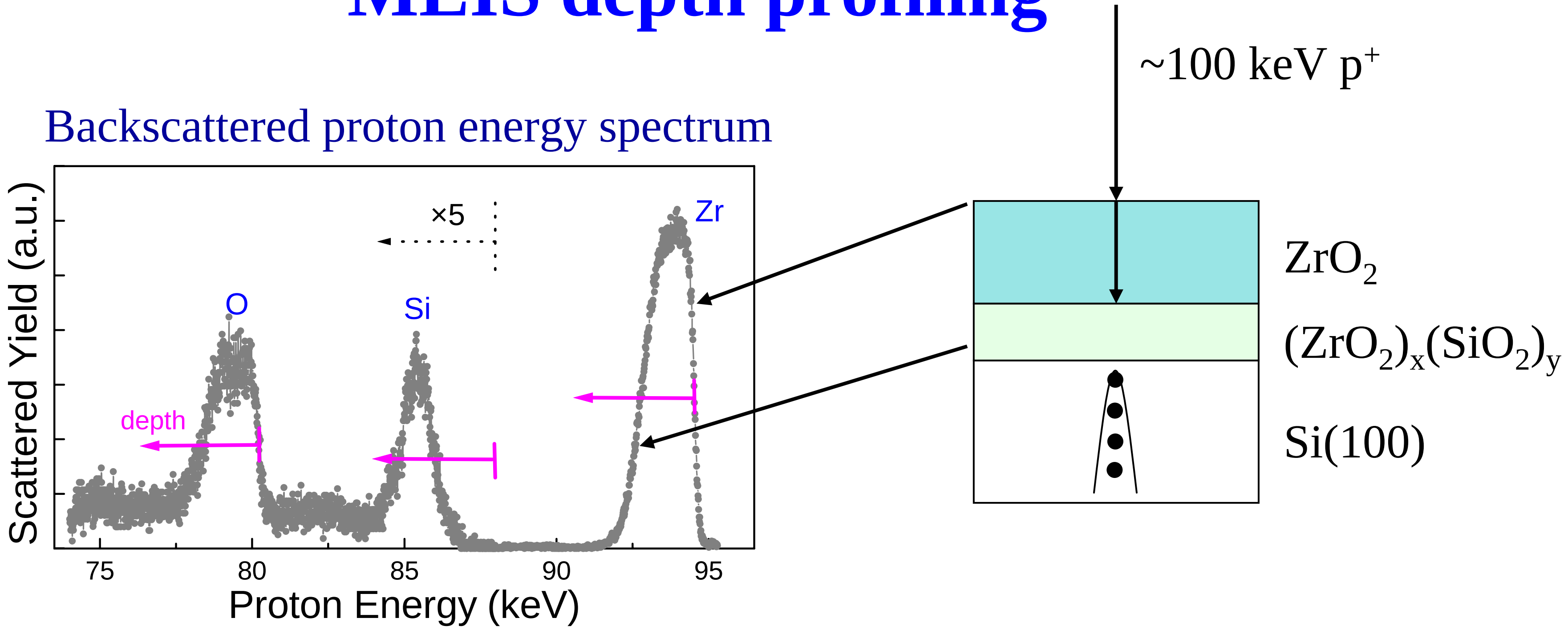
Backscattered proton energy spectrum

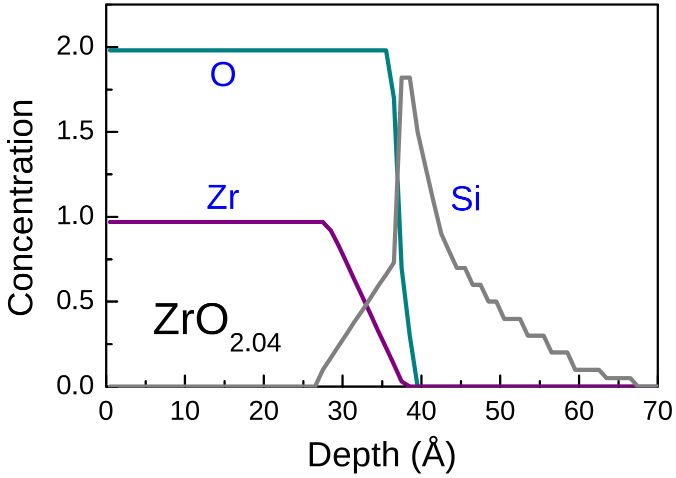
depth profile

- **Sensitivity**:
  ≈ 10^{+12} atoms/cm² (Hf, Zr)
  ≈ 10^{+14} atoms/cm² (C, N)
- **Accuracy** for determining total amounts:
  ≈ 5% absolute (Hf, Zr, O), ≈ 2% relative
  ≈ 10% absolute (C, N)
- **Depth resolution**: (need density)
  ≈ 3 Å near surface
  ≈ 8 Å at depth of 40 Å

Rutgers MEIS work on CMOS gate stack

- Film stoichiometry and thickness for multilayer structures
- Interface properties (e.g. composition and thickness)
- Film initiation and growth (esp. ALD)
- Influence of barrier layers (e.g. nitride diffusion barrier)
- Thermal stability (silicate and silicide formation, decomposition)
  - Si, Ge, GaAs, SiC substrates
- Atomic mobility (O, Si, metal, impurity…)
- Impurities – C, H, As…
- Epitaxial oxides - e.g. STO/Si
- Metal electrode/high-K dielectric interface

Interface control: SiO_2 content by MEIS

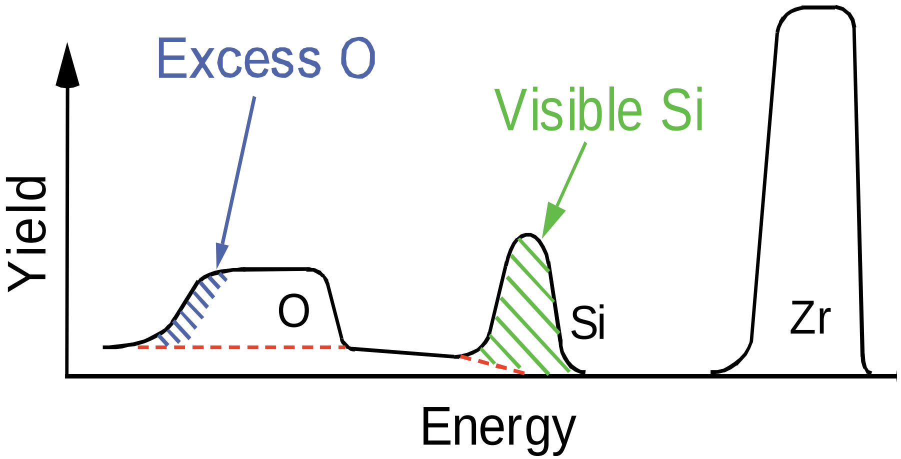

Interfacial SiO_2 may be quantified by:

Measure excess oxygen O_{ex} (beyond that needed in oxide) at interface.

Measure total number of *visible* Si atoms $\Delta t_{SiO_2} = (Si_V - 8.3) \times 2.7Å$

Model/deconvolute MEIS energy spectrum

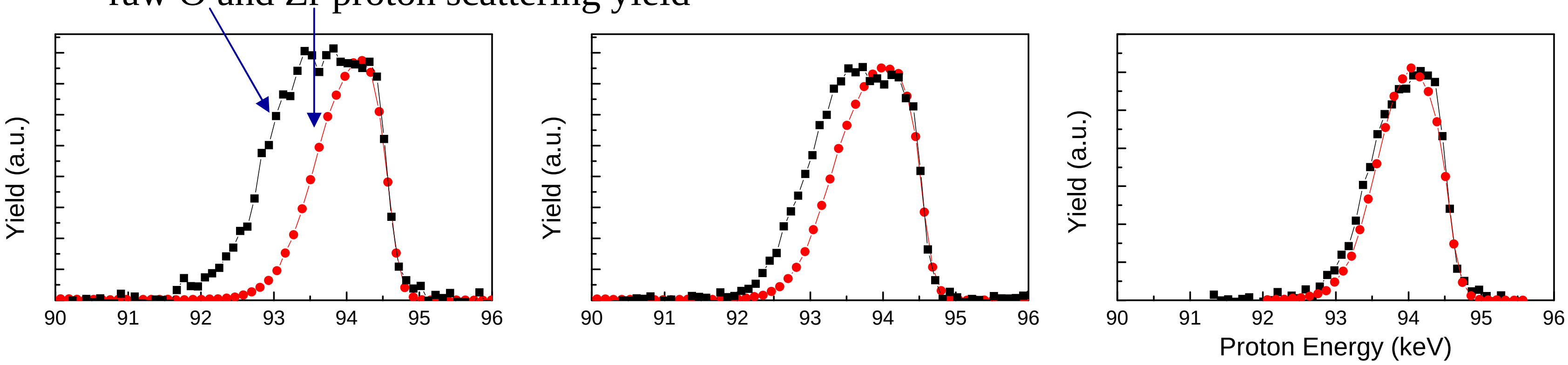
raw O and Zr proton scattering yield

- Normalize O and M peak position (to surface scattering energy) and heights.
- Can use to quantify excess (or missing) O in raw data
- $ZrO_2/SiO_2/Si$ –process-dependent interface SiO_2 thickness

MEIS spectra of La silicate with air and vacuum anneals

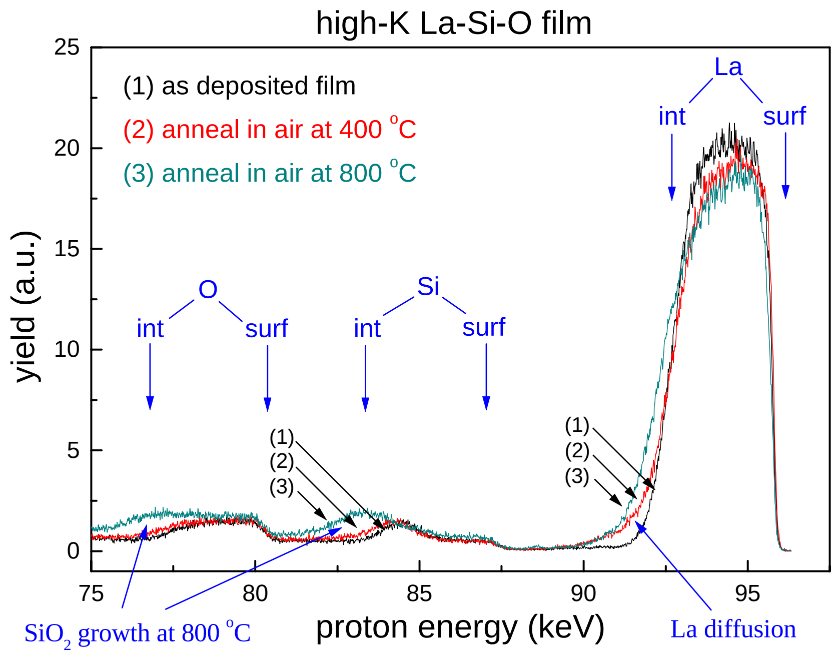

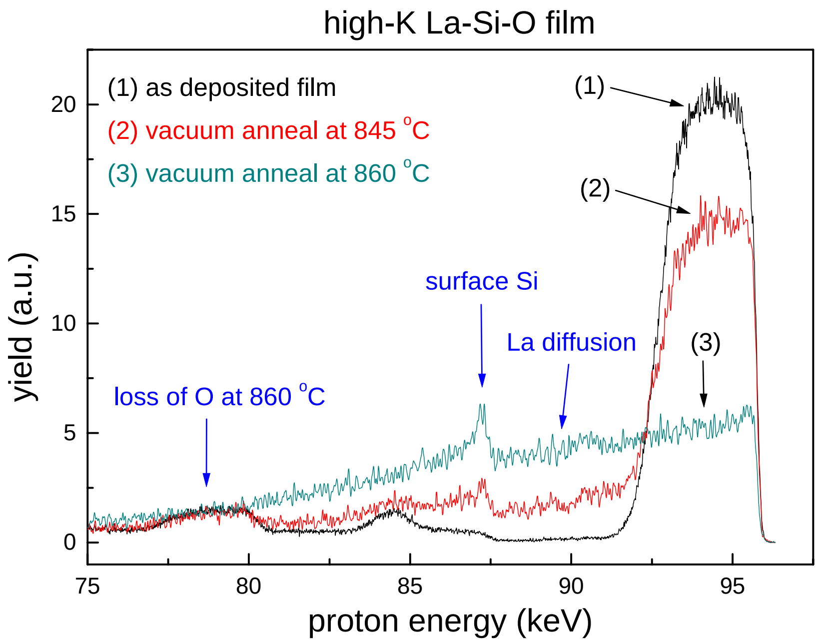

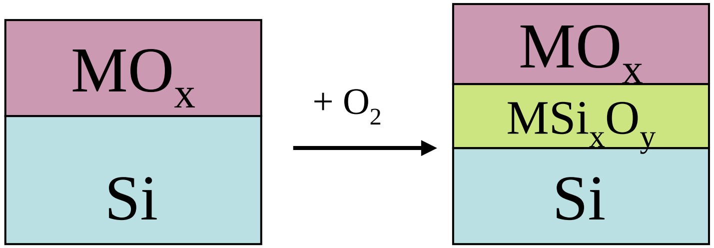

$MO_x + Si \Rightarrow MSi_y + SiO\ (g)$

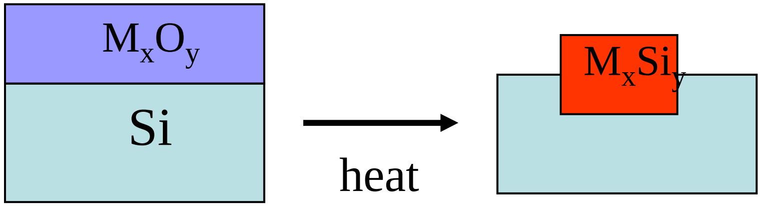

- Vacuum anneal – no change until T>800C, then decomposition
- Atmospheric anneal – growth of silicate at interface

Post-process in reducing atmosphere

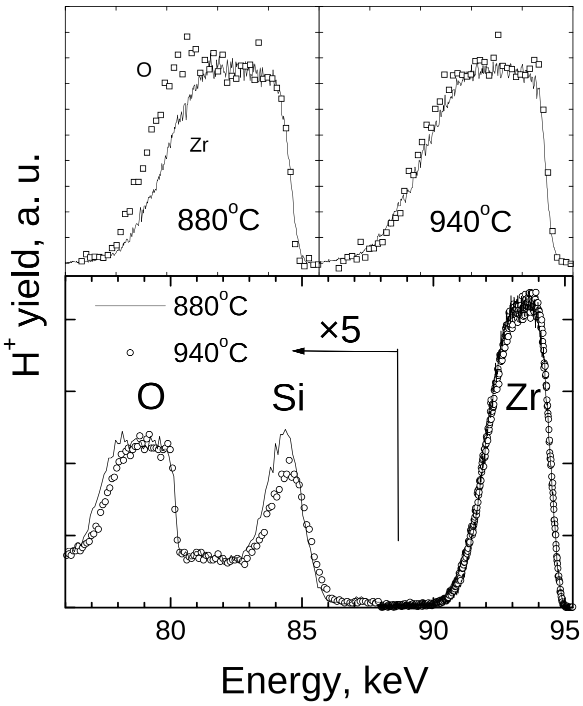

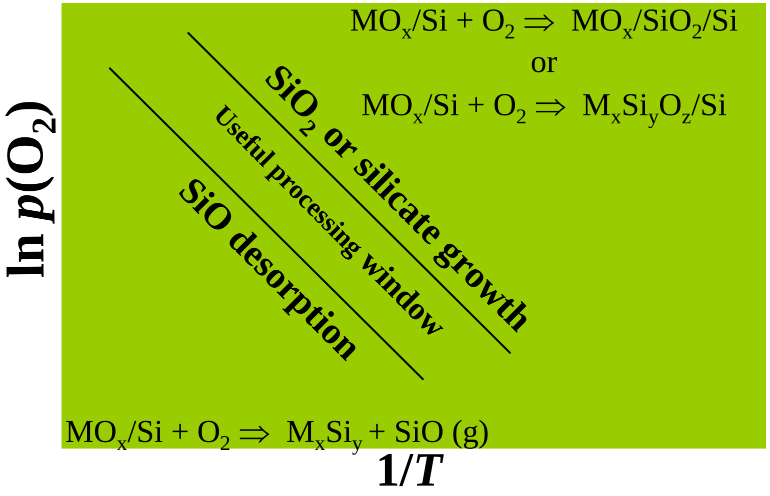
$MO_x/Si + O_2 \Rightarrow MO_x/SiO_2/Si$

or

$MO_x/Si + O_2 \Rightarrow M_xSi_yO_z/Si$

$MO_x/Si + O_2 \Rightarrow M_xSi_y + SiO\ (g)$

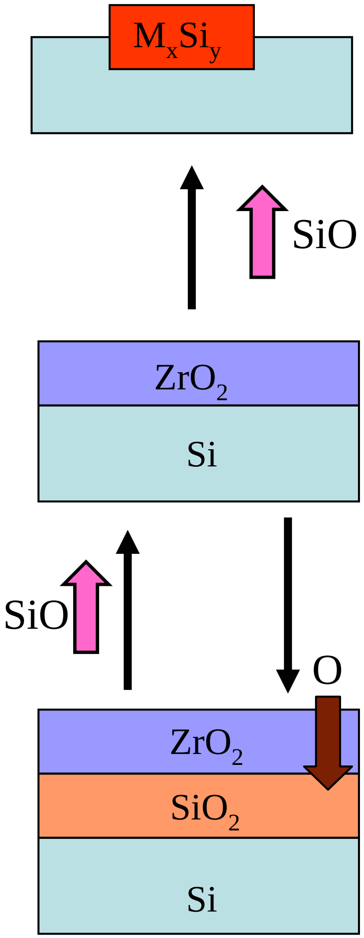

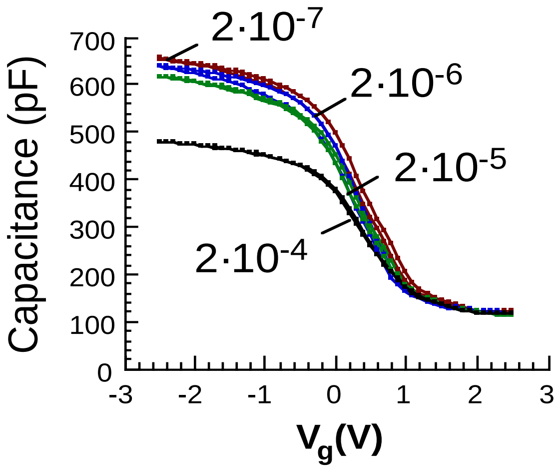

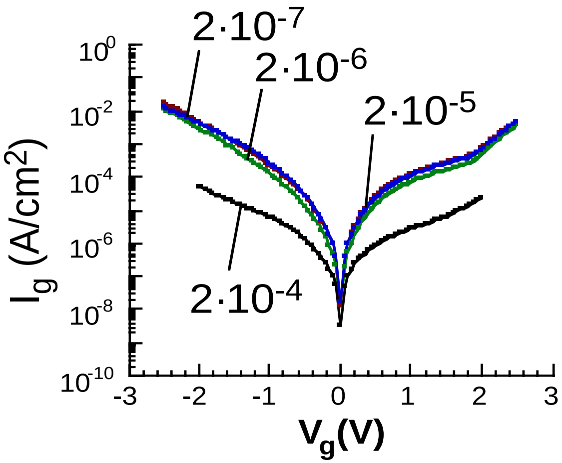

Decomposition schemes for $HfO_2/SiO_2/Si$ gate stack

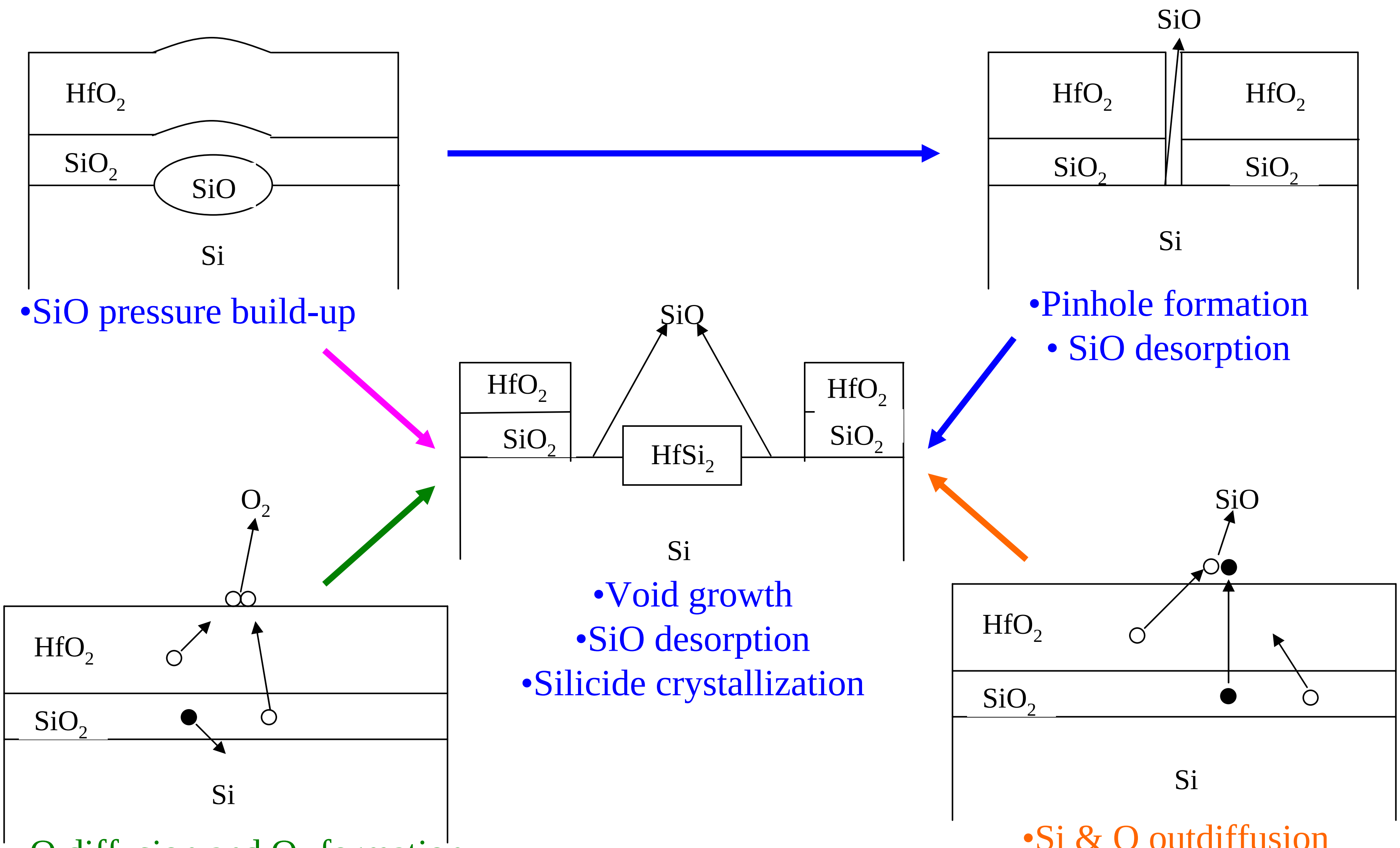

- SiO pressure build-up

- Pinhole formation
- SiO desorption

- Void growth
- SiO desorption
- Silicide crystallization

- O diffusion and O_2 formation
- Hf and/or Si oxide reduction

- Si & O outdiffusion
- SiO desorption
- SiO_2 thinning

Behavior of La, Y, Gd, Ce … oxides upon exposure to atmosphere and annealing

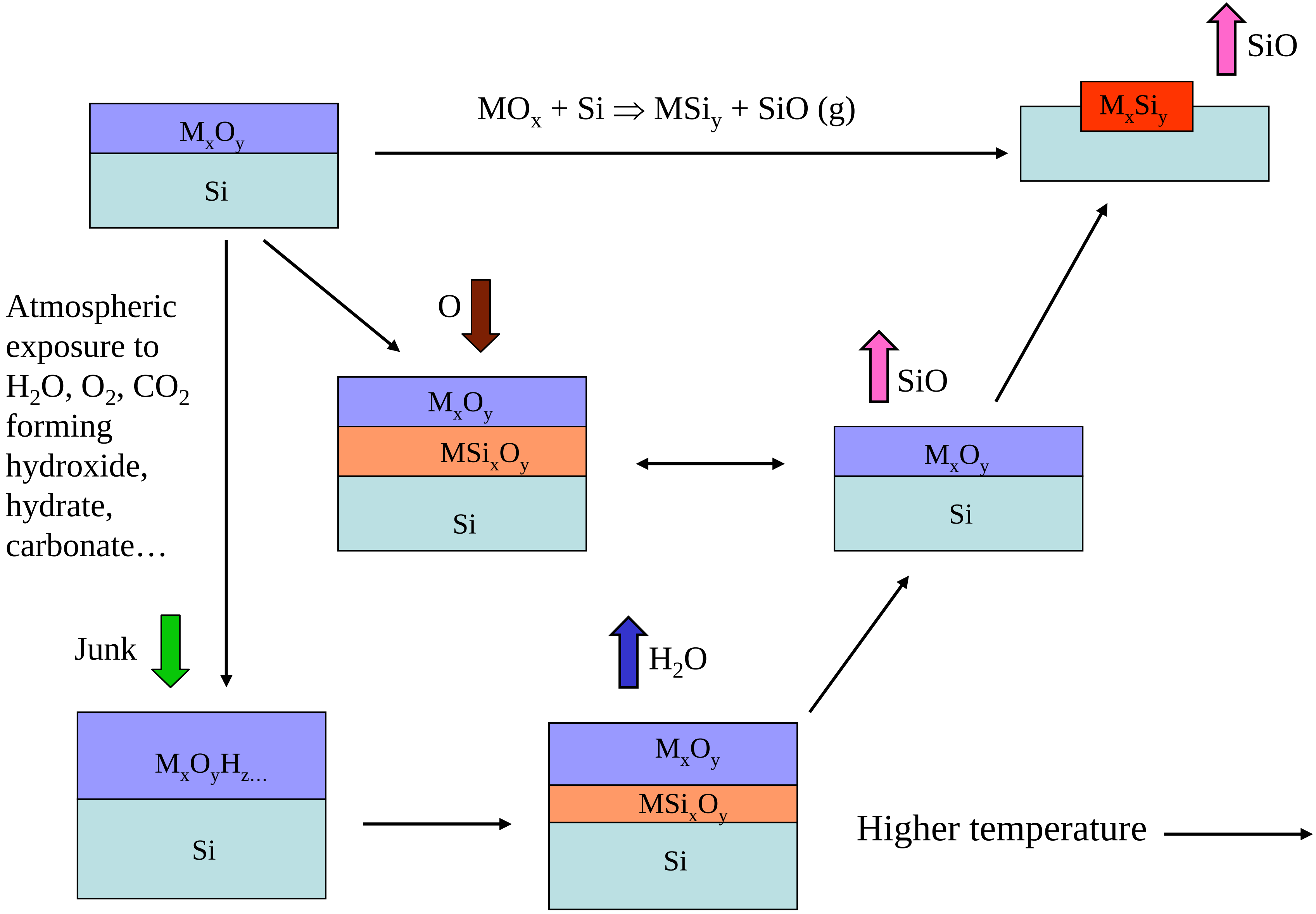

$MO_x + Si \Rightarrow MSi_y + SiO\ (g)$

Atmospheric exposure to H_2O, O_2, CO_2 forming hydroxide, hydrate, carbonate…

Higher temperature →

One approach to interface control: Grow in UHV

MEIS spectra for MBE grown HfO_2 on Si(001) after UHV anneals

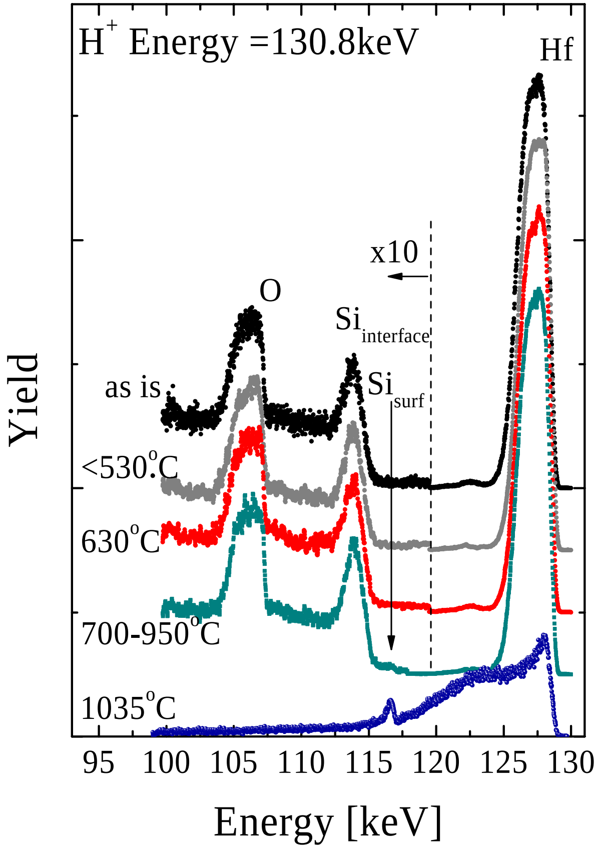

- ✓ No SiO_2 layer on HfO_2/Si interface, stable to anneal in UHV to ≲530°C
- ✓ growth of thin (~4Å) SiO_2 interfacial SiO_2 layer at T~630°C
- ✓ complete film disintegration only above ~1020°C
- ✓ Broadening of the O peak and a small increase of the Si peak indicate interfacial SiO2 formation

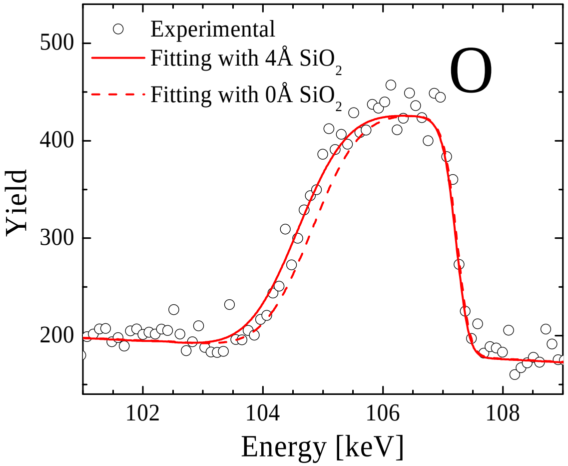

(with R. Kwo, National Tsing Hua University, Taiwan)

Isotope studies of diffusion in oxides

Oxygen (O_2) transport in SiO_2

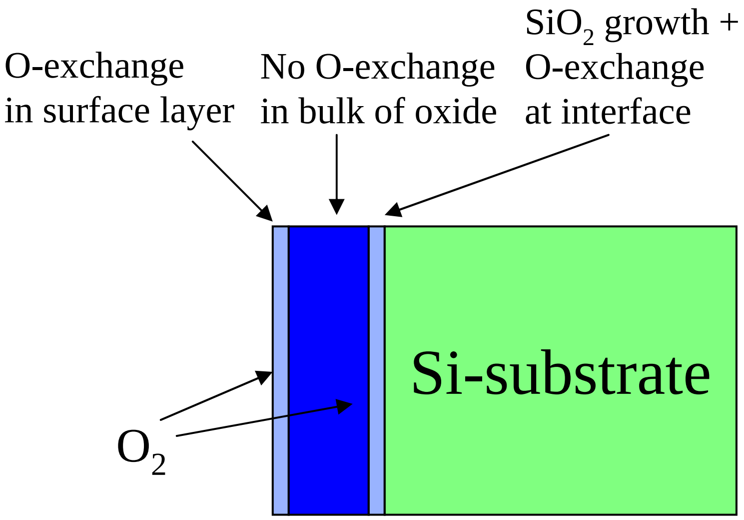

O-exchange in surface layer

No O-exchange in bulk of oxide

SiO_2 growth + O-exchange at interface

Si-substrate

O_2

Atomic oxygen (O) transport in high-K films

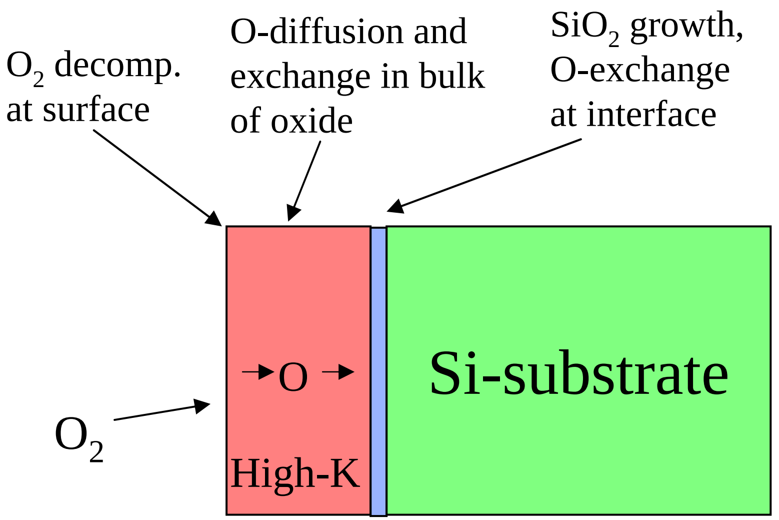

O_2 decomp. at surface

O-diffusion and exchange in bulk of oxide

SiO_2 growth, O-exchange at interface

→O →

High-K

Si-substrate

O_2

<u>SiO_2 films:</u>

- amorphous after annealing
- molecular O_2 transport in SiO_2
- decomposition by SiO desorption

<u>High-K films (except Al_2O_3):</u>

- tend to crystallize at low T
- high oxygen mobility

Isotope tracer studies

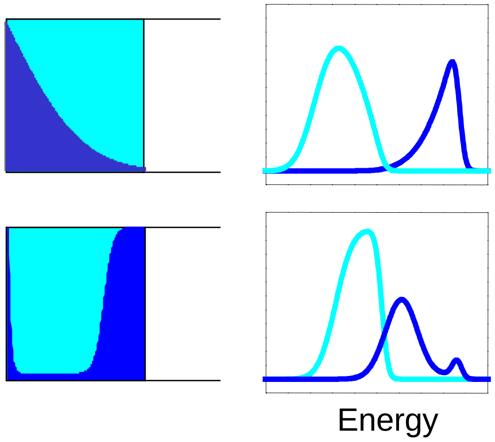

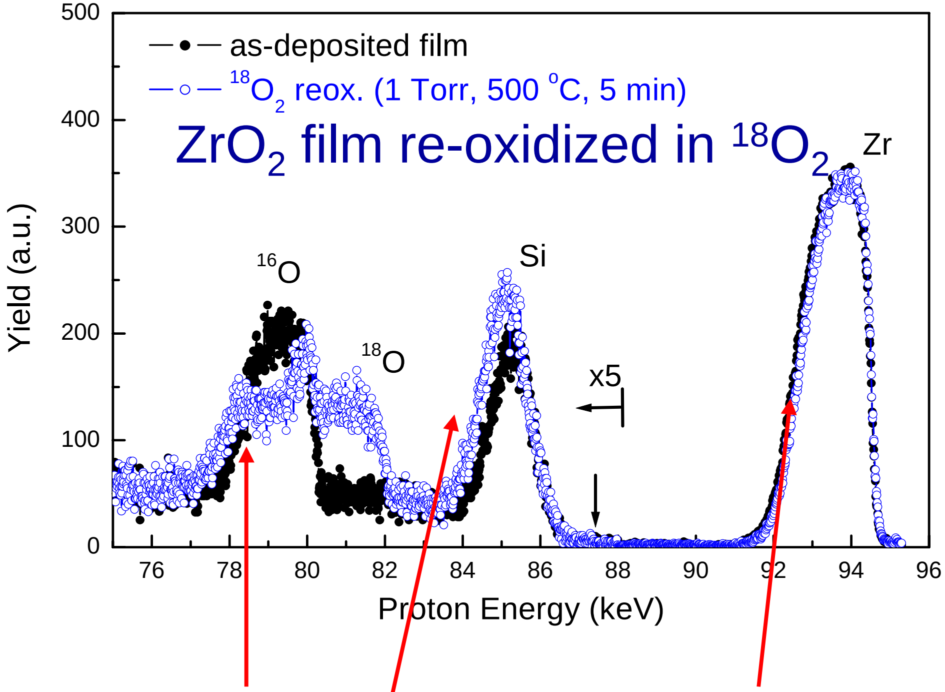

Deeper O and Si

No change in Zr profile
Surface flat by AFM

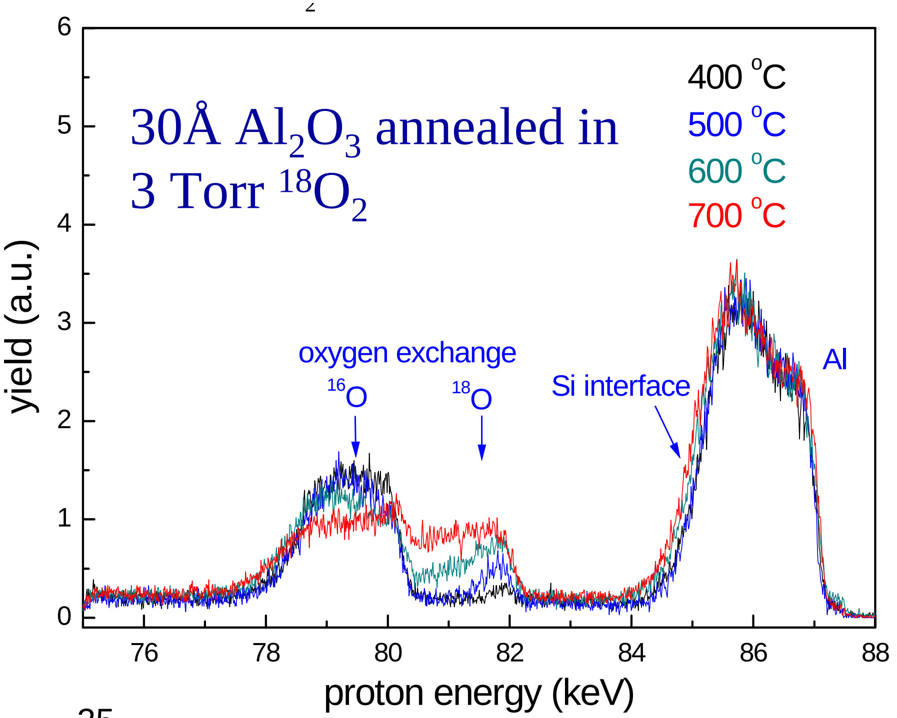

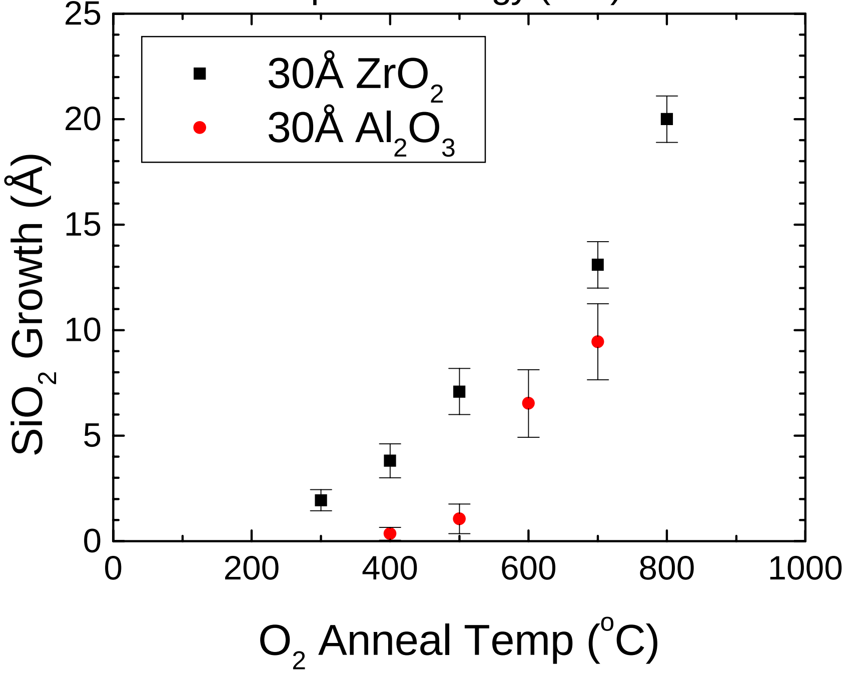

- Significant interfacial SiO_2 growth for ZrO_2, less for Al_2O_3
- Dramatic oxygen exchange:
  ^{18}O incorporation and ^{16}O removal
- SiO_2 growth rate faster than DG-like growth (O_2 on Si)
- Growth faster under ZrO_2 than Al_2O_3

Isotope reactions and diffusion in silicates

Relation between composition and O incorporation (addition and exchange)

$HfO_2(SiO_2)_x$ re-oxidation in ^{18}O: 500° C, 10^{-2} Torr, 30 min

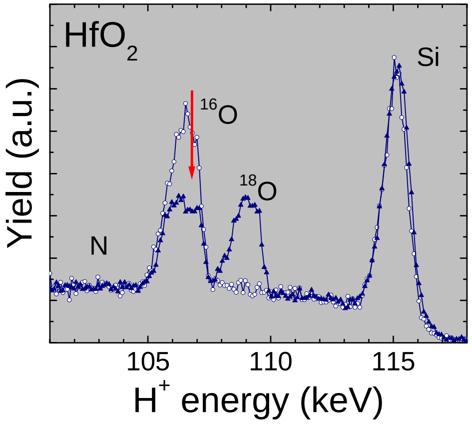

x = 0%

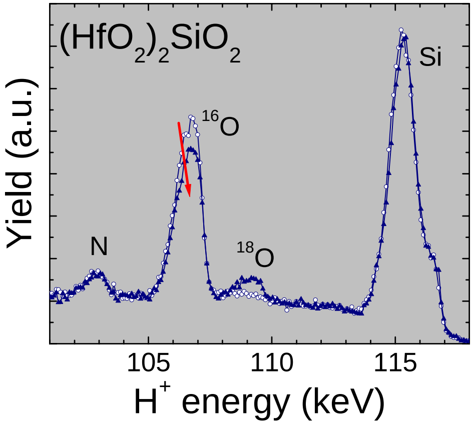

33%

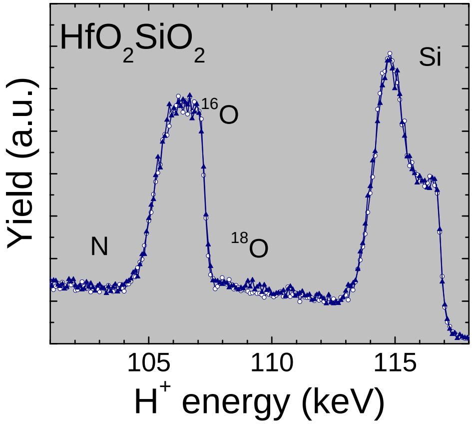

50%

- strong exchange reaction even at 500°C: ^{16}O loss, but the same total O concentration
- no change in width of ^{16}O and Si peaks (no formation of interfacial oxide)
- exchange rate decreases with increase of SiO_2 fraction *x*
- 50% of SiO_2 in $HfO_2(SiO_2)_x$ is enough for almost full suppression of oxygen exchange

Rutgers/Sematech

Oxygen interaction with cerium oxide

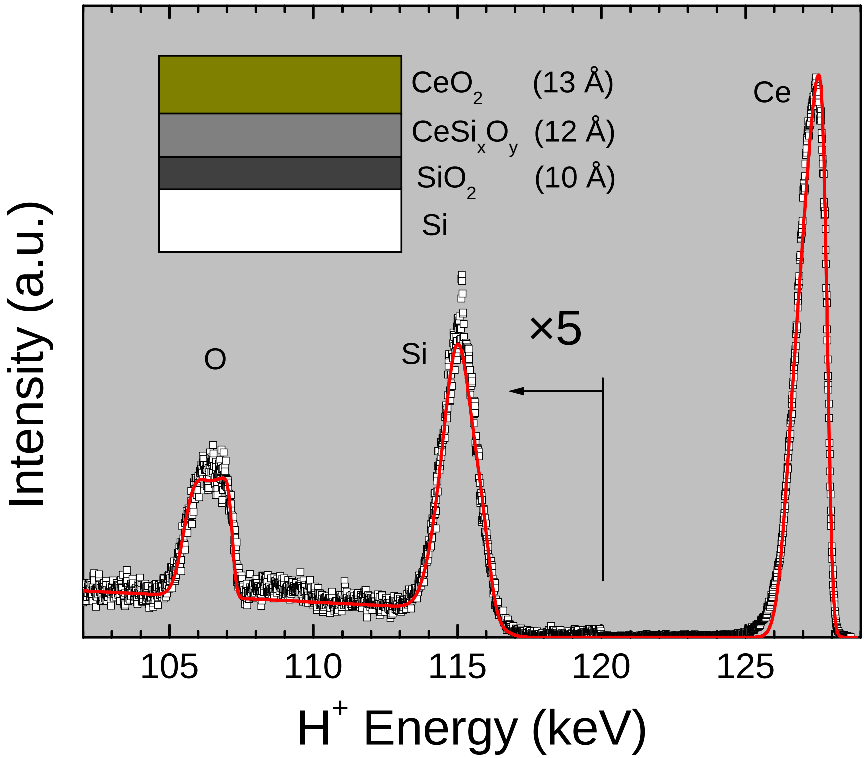

Sample I: as-grown

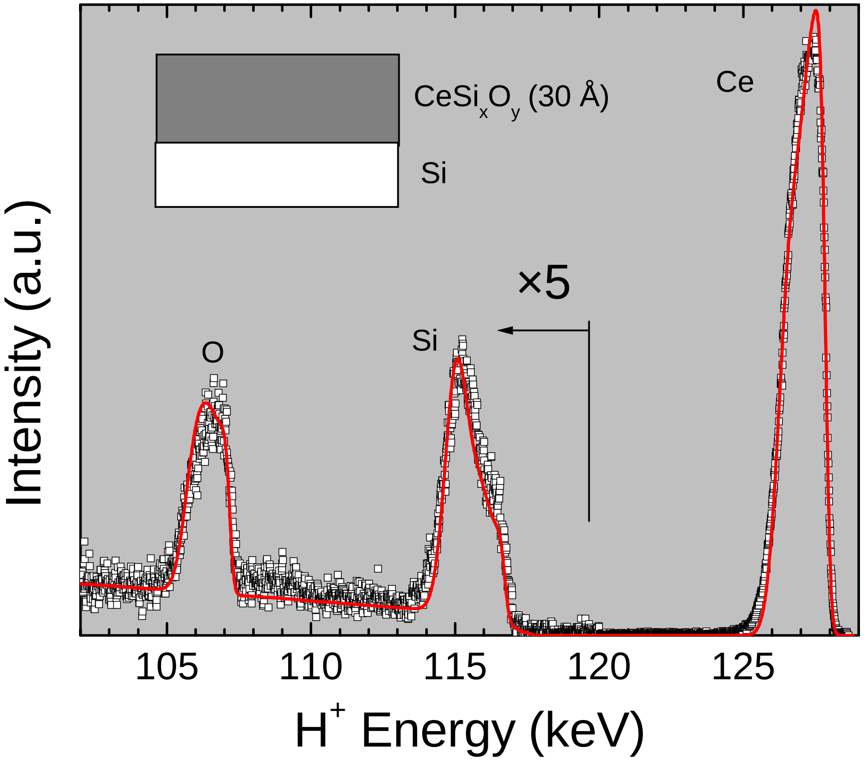

Sample II: Sample I annealed to 750°C 10 min

- interfacial Ce^{4+} is reduced to Ce^{3+} state
- interfacial SiO$_2$ and silicate

- dissolution of interfacial SiO$_2$ with formation of a thick silicate film

Isotopic study of Ce oxide re-oxidation

10^{-2} torr $^{18}O_2$, 500° C, 15 min H^+ 130.75keV; 125.3°

Sample I "Ce oxide"

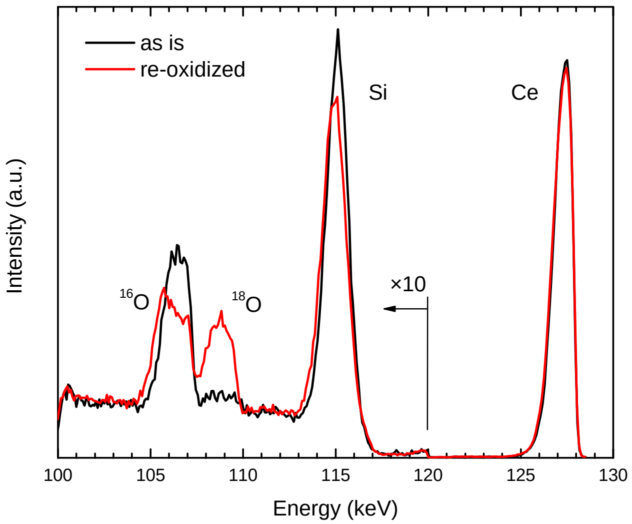

Sample II: Ce silicate

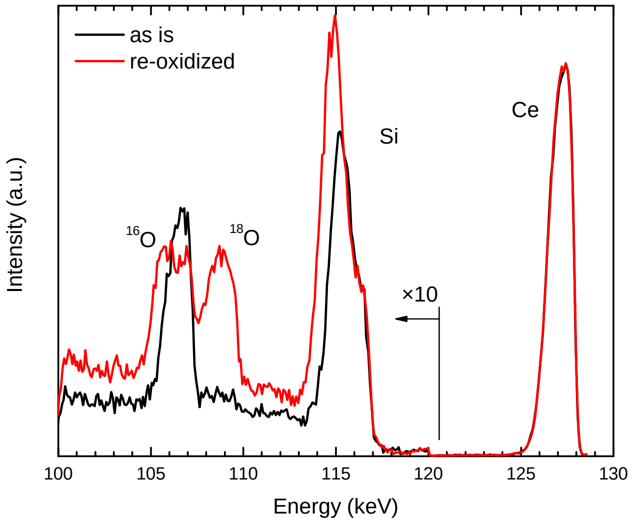

- the oxygen content in the films increases upon re-oxidation for both samples
- much more rapid interface growth than Hf silicate case
- the Si yield increases <u>for the silicate</u>, consistent with SiO_2 formation
- broadening and lowering of ^{16}O peak suggests oxygen transport via place exchange mechanism

Use barrier monolayers to minimize diffusion and interface reactions

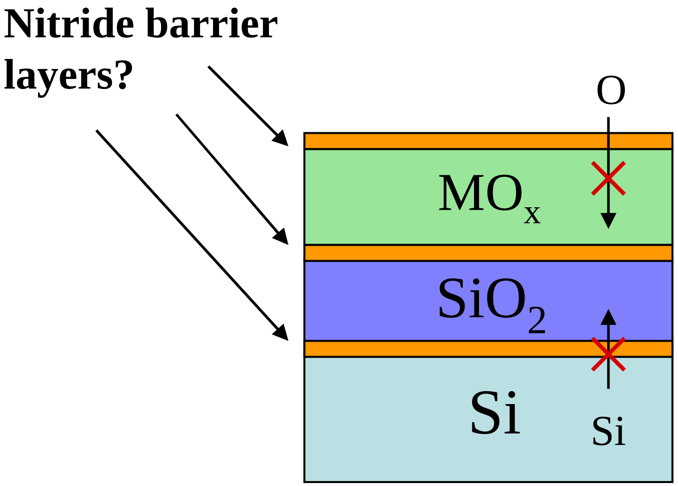

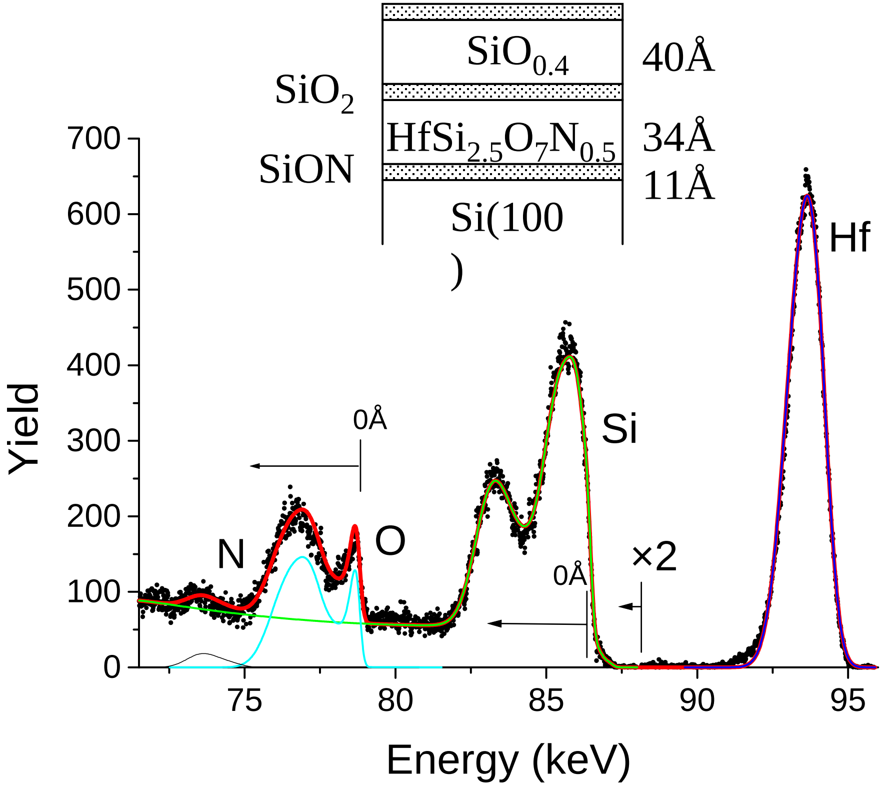

- **Nitride barrier layers helpful to slow O, Si and dopant diffusion, as well as silicate formation and other interface reactions.**
- **Nitridation also raises crystallization temperature.**

w/Wallace

MEIS of Al_2O_3 on GaAs

No etch

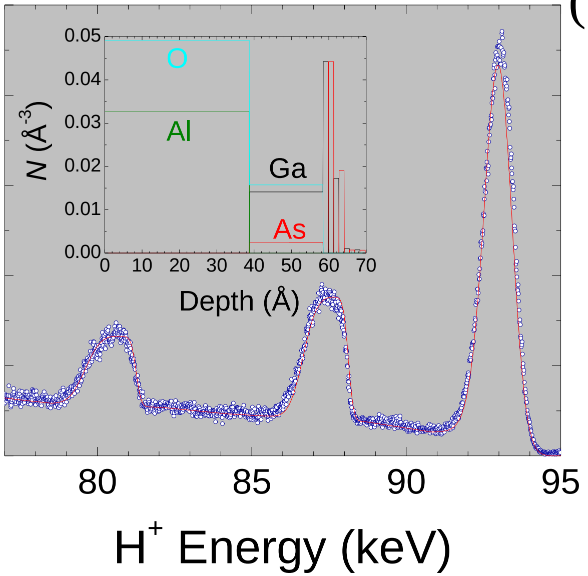

<u>Interfacial oxide:</u>

$(Ga_2O_3)_{0.37}(Ga_2O)_{0.63}(As_2O_3)_{0.17}$, porous oxide: $\rho = 0.5\ \rho_{bulk}$
(see poster for reasoning)

	n(Ga+As), Å^{-2}	*n(Al), Å^{-2}*	*n(O), Å^{-2}*	*n(O)/n(Al)*
HF etch	0.33	1.48	2.23	1.51
No etch	0.55	1.30	2.22	1.70

- interfacial oxide is much thinner for the HF-etched sample

- Weak contrast difference between Al_2O_3 and Ga_xAs_yO.

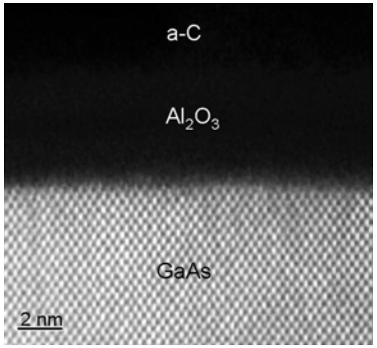

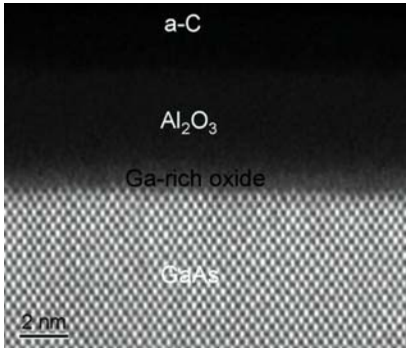

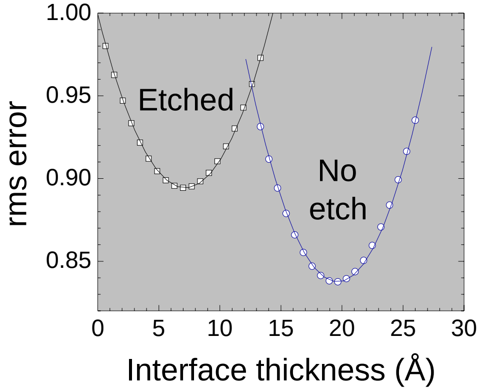

A one parameter fit

w/Agere

HfO_2 on GaAs: MEIS and TEM comparison

	TEM*	MEIS
No etch	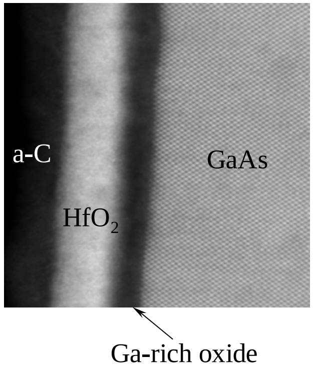	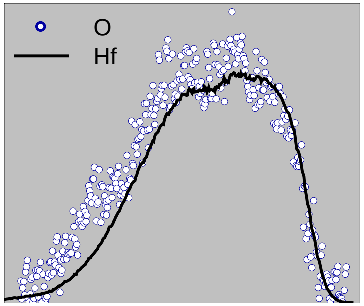
HF etch	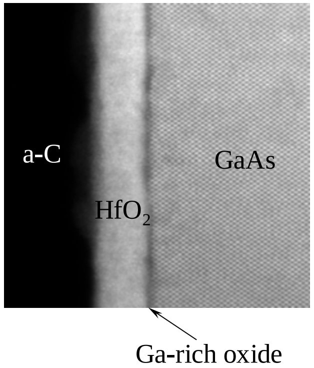	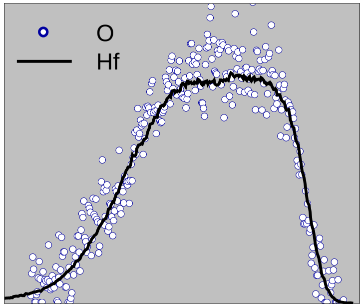

- TEM and MEIS results are consistent;
- native oxide ≈ 20 Å;
- As:Ga ≈ 0.17, (Ga+As):O ≈ 1.04

w/Agere

Epitaxial $SrTiO_3$ on Silicon

An ideal problem for MEIS: composition and structure in a thin film (heavy Z on light Z substrate)

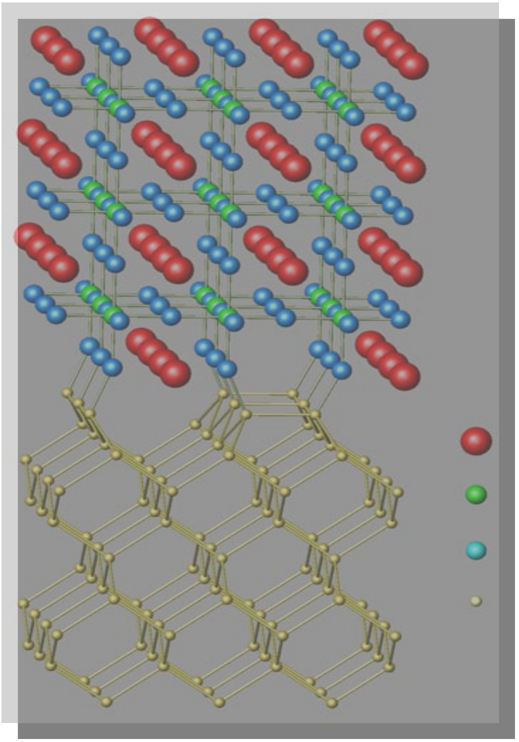

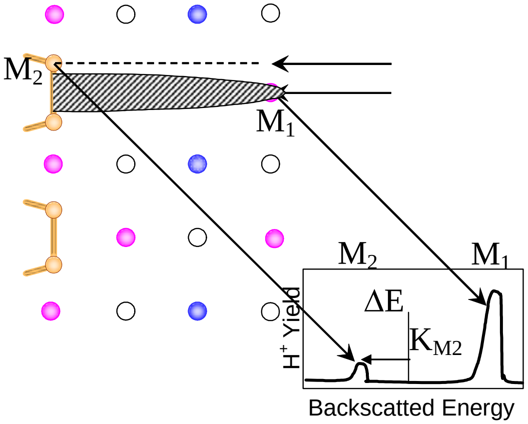

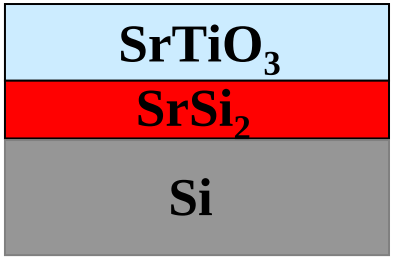

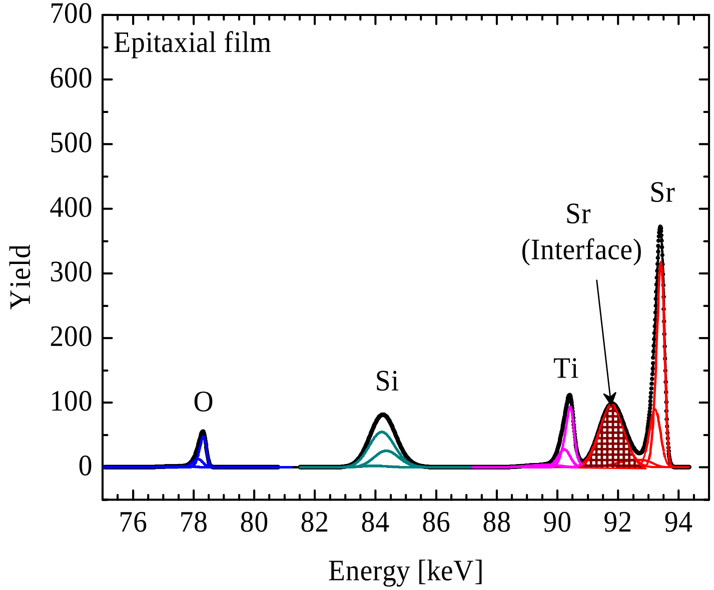

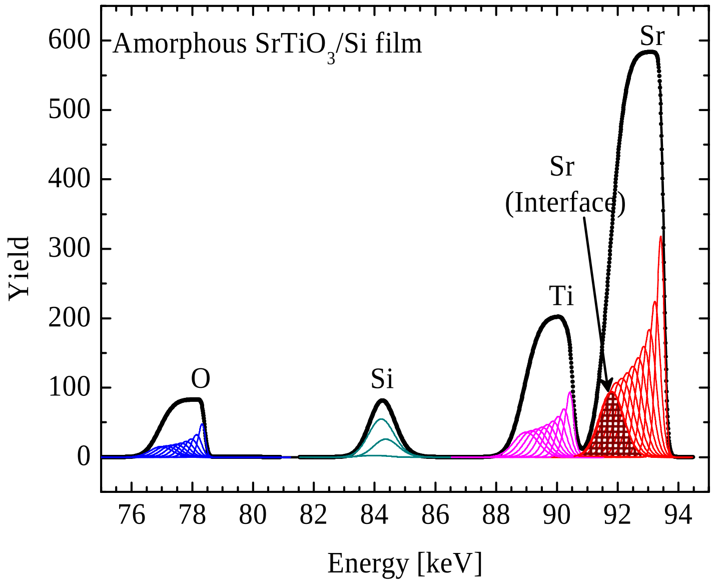

Inspired by McKee, Schlom, Chambers, Motorola …

Normal incidence, 98keV H^+, scattering angle 125° (substrate Si blocking)
$SrTiO_3/SrTiSi_xO_y/Si(001)$

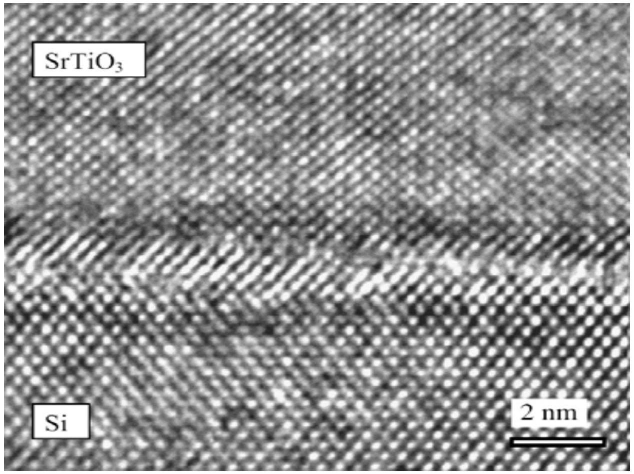

High-resolution TEM image of the interface between the $SrTiO_3$ film and Si(001)

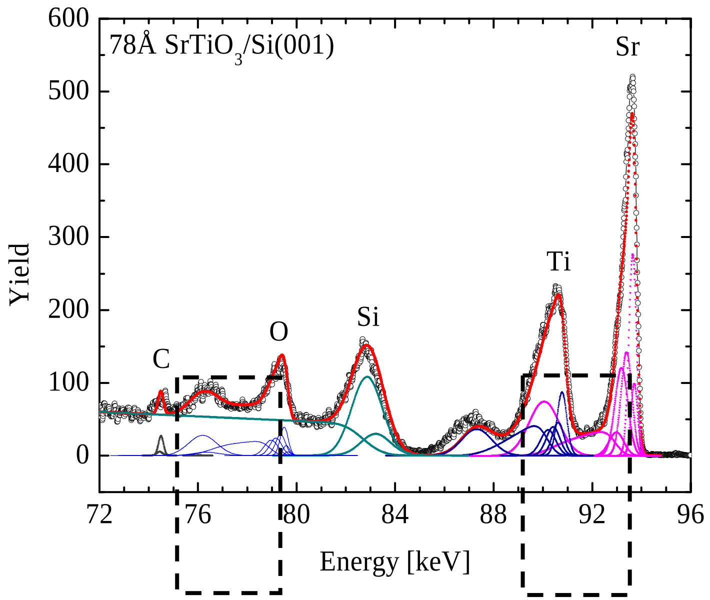

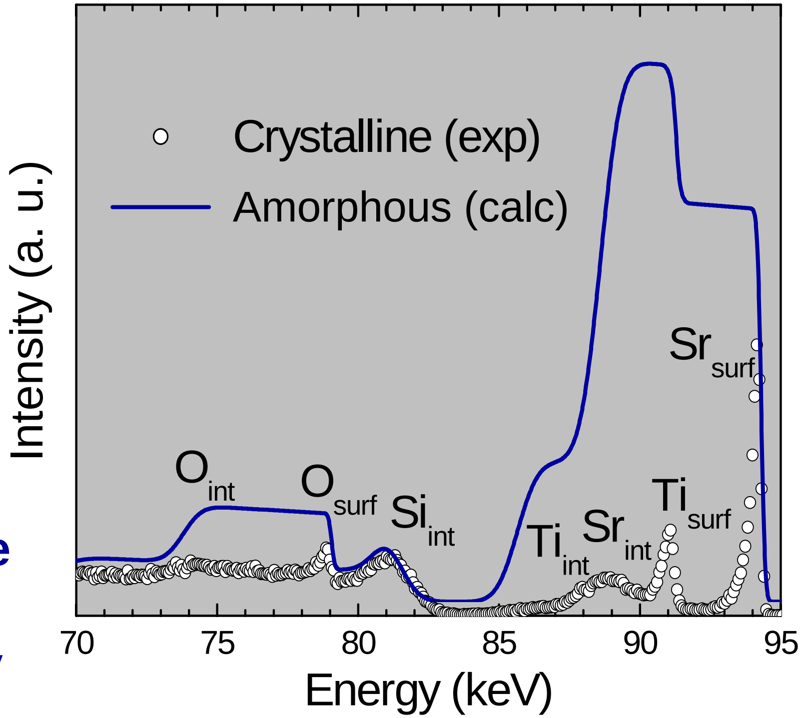

Sr, Ti and O are observed in the interface region - they are visible to the ion beam (not blocked) in this scattering geometry

Ion scattering studies of metallization

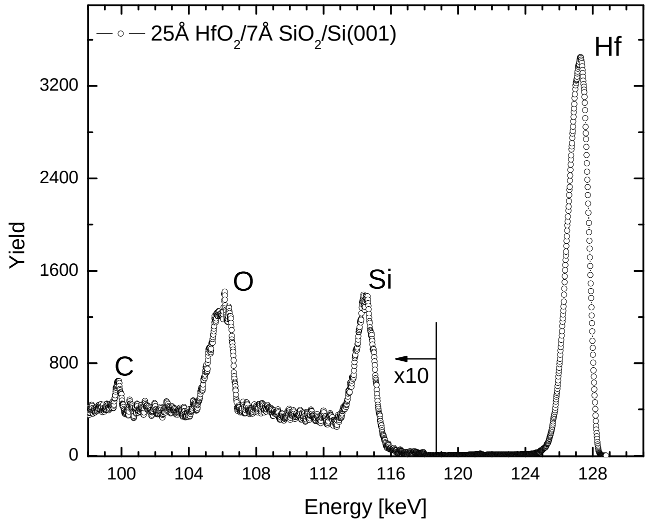

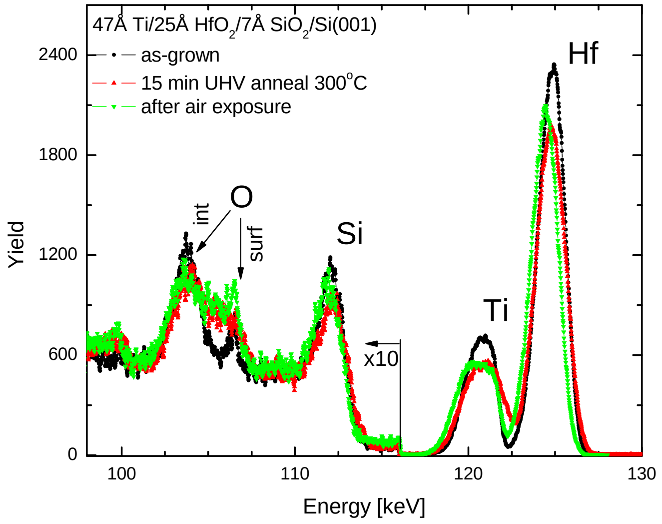

1. Initial HfO_2 film has small amount of interfacial SiO_2 (~6-7Å);
2. Deposited Ti forms uniform in thickness layer, no intermixing with HfO_2; very low oxygen concentration in Ti layer.
3. Lowering and broadening of Ti peak after UHV anneal at 300°C indicate Ti oxidation
4. After air exposure (room temperature) further O intake in Ti is observed

Initial stack composition

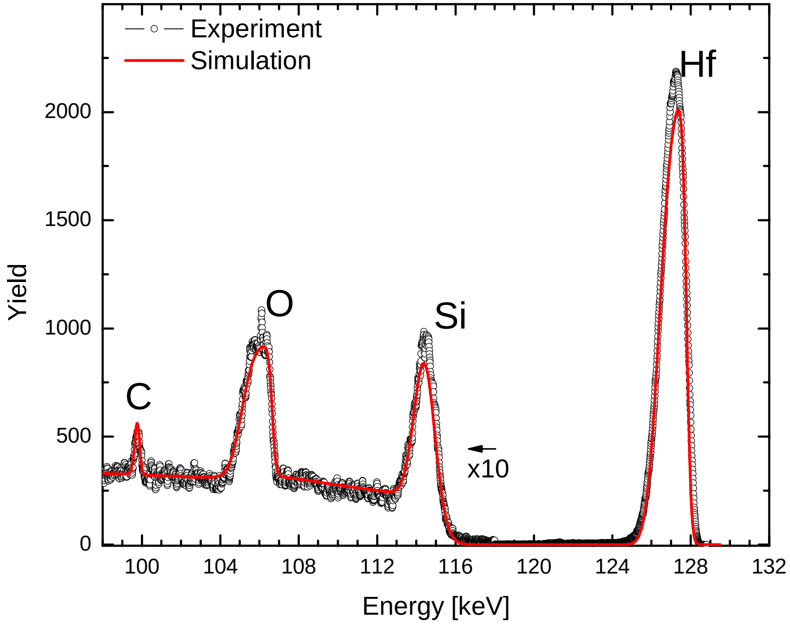

- There is small amount of SiO_2 on the interface.
- HfO_2 stoichiometry is very close to Hf:O = 1:2
- Note C on the topmost surface ([C]=2.6x10^{15}[atoms/cm^2])

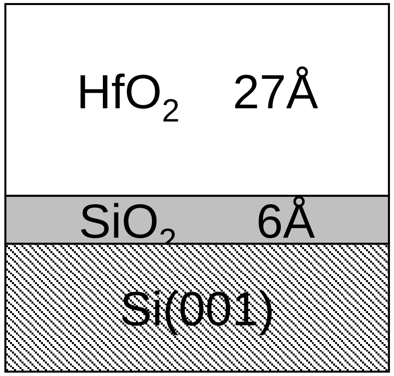

HfO_2 27Å

SiO_2 6Å

Si(001)

Concentration	X10^{15}[atoms/cm^2]
Hf	7.48
O	14.95+2.65=17.60

Ti deposition *in situ*

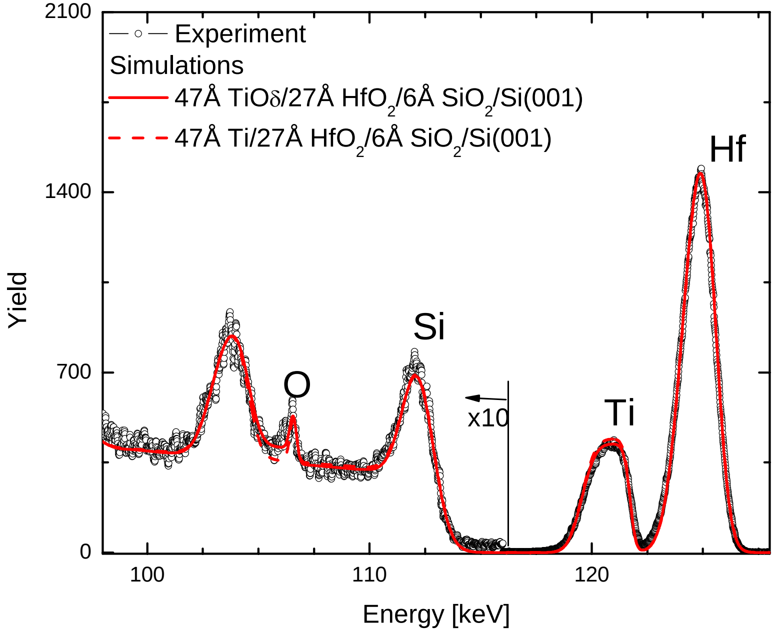

- ~45Å Ti was deposited at RT and p=1×10^{-7} Torr;
- MEIS measurements were done in 14 hrs after deposition
- there is a small oxygen concentration in the Ti layer
- however simulations indicate that there is still visible amount of SiO_2 remaining on the HfO_2/Si(001) interface

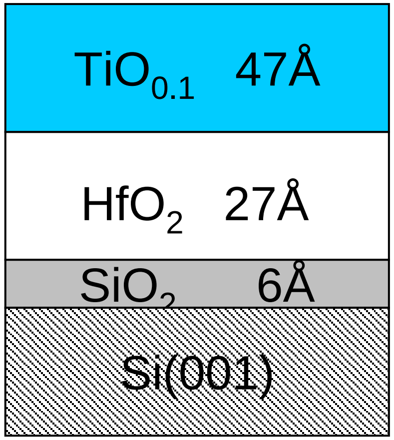

$TiO_{0.1}$ 47Å

HfO_2 27Å

SiO_2 6Å

Si(001)

Concentration	X10^{15}[atoms/cm^2]
Ti	1.93+21.36+2.00=25.3
Hf	7.48
O O in surface TiOx	14.95+2.65=17.60 1.93

Possible intermixing on the Ti-HfO_x interface

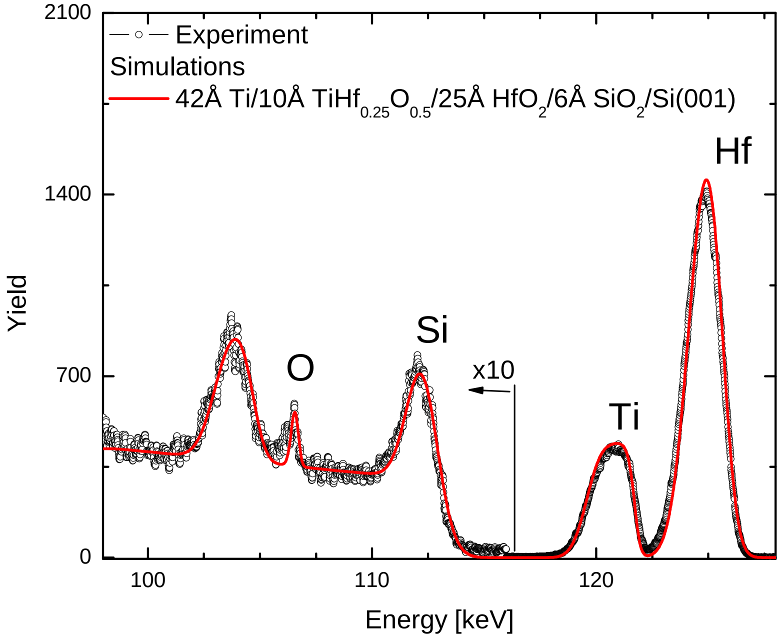

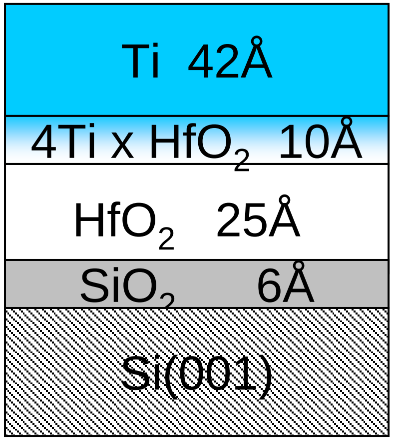
Ti 42Å

4Ti x HfO_2 10Å

HfO_2 25Å

SiO_2 6Å

Si(001)

Initial high concentration of C on the surface prior to Ti deposition makes modeling of the Ti – HfO_2 interface far away from ideal, mixing between Ti and HfO_2 is possible

UHV anneal to 300ºC

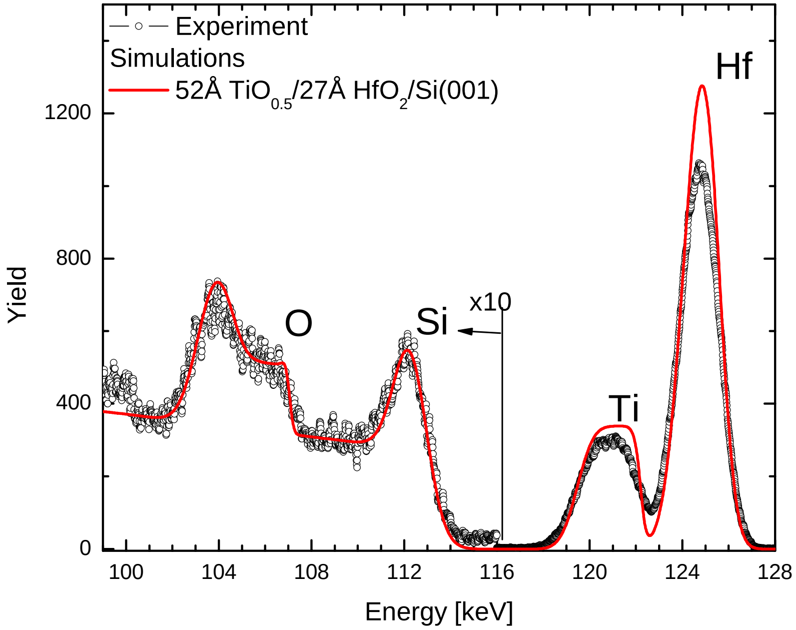

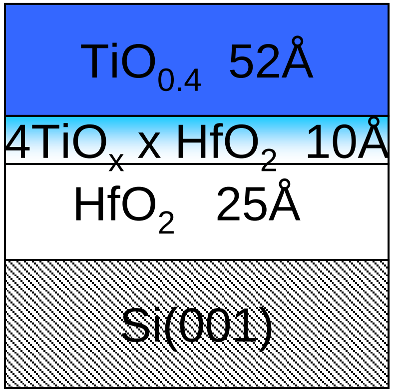

$TiO_{0.4}$ 52Å

$4TiO_x$ x HfO_2 10Å

HfO_2 25Å

Si(001)

Lowing and broadening of Ti peak with growth of O yields for the Ti region indicate Ti oxidation

Decrease of Si surface peak and decrease of the width of O peak indicate possible removal of SiO_2 layer

MEIS of $Ta/La_2O_3/Si$

H^+ Incident energy 130.8 keV, scattering angle=125°

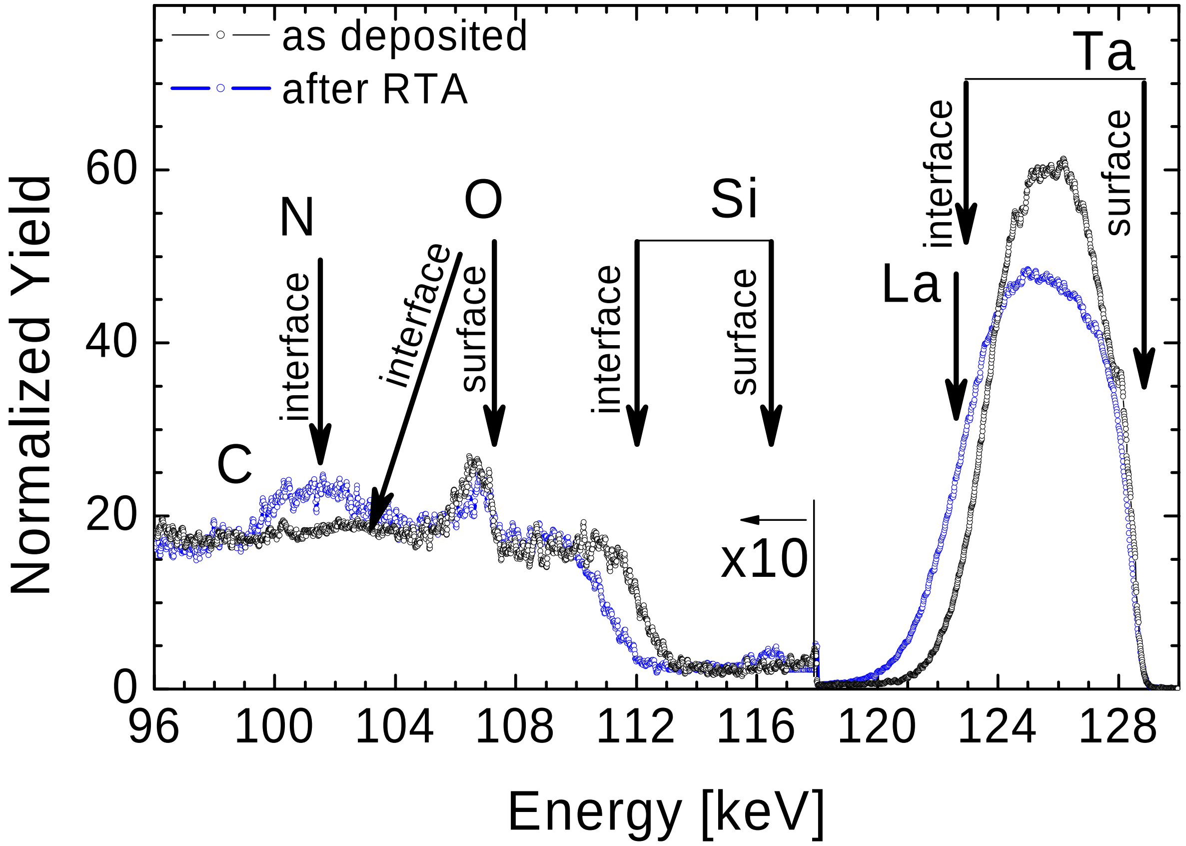

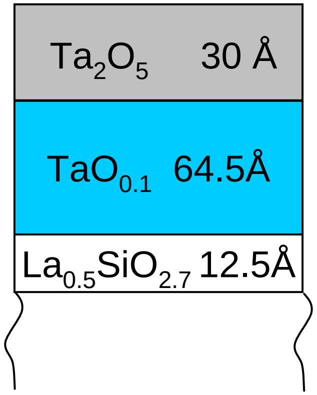

Ta_2O_5 30 Å

$TaO_{0.1}$ 64.5Å

$La_{0.5}SiO_{2.7}$ 12.5Å

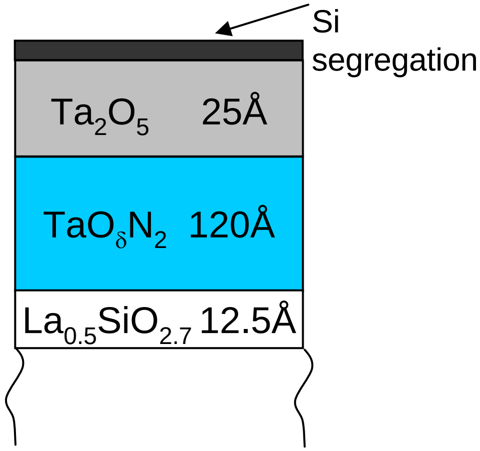

Si segregation

Ta_2O_5 25Å

$TaO_\delta N_2$ 120Å

$La_{0.5}SiO_{2.7}$ 12.5Å

- **8nm Ta on 1nm La2O3 (no mass separation between Ta and La)**
- **Nitrogen signal grows in RTN; no clear interfacial SiO2 growth**

Rutgers/NCSU

$La_2O_3/SiO_2/Si$ (no Ta cap)

H^+ Incident energy 130.8 keV, scattering angle=125°

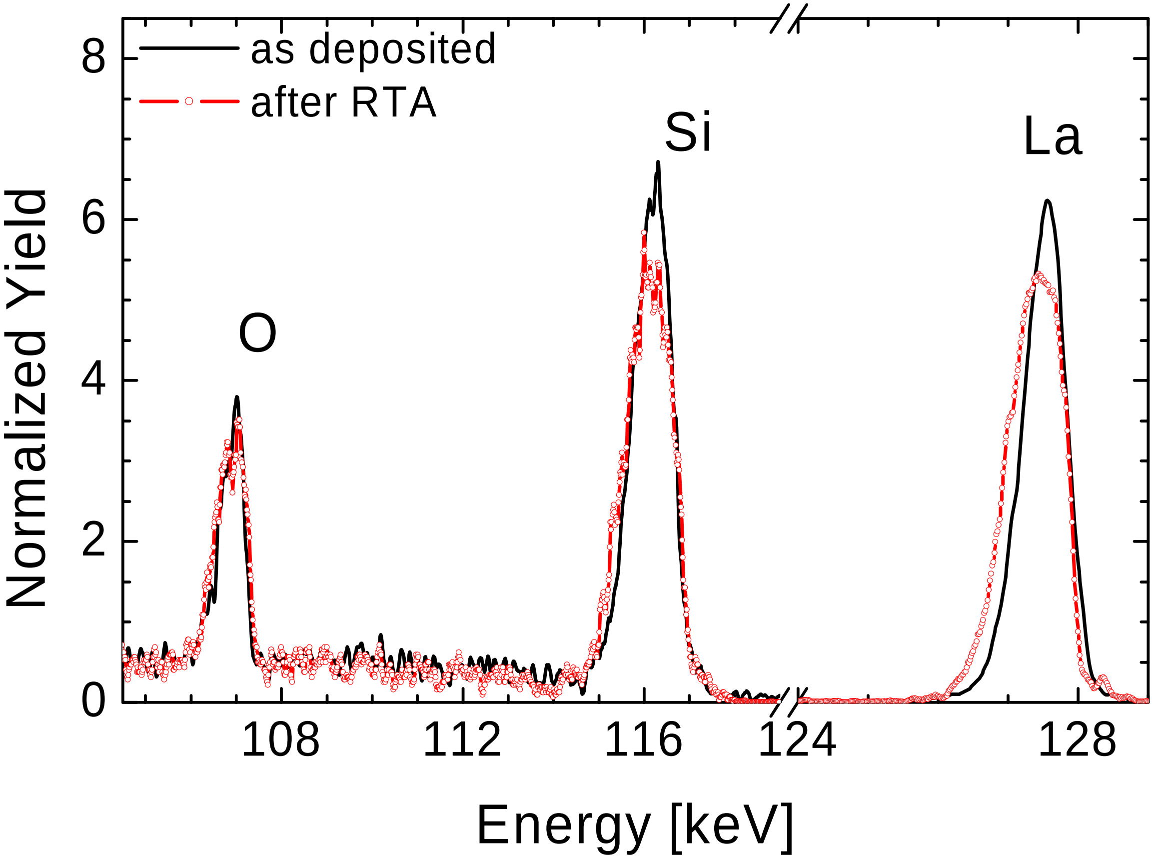

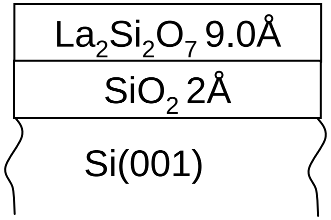

One model of the as-deposited film

- **RTN to 1000A; no nitrogen dissociation or oxide growth**

Rutgers/NCSU

MBE grown 5nm Sc_2O_3/Si(111)

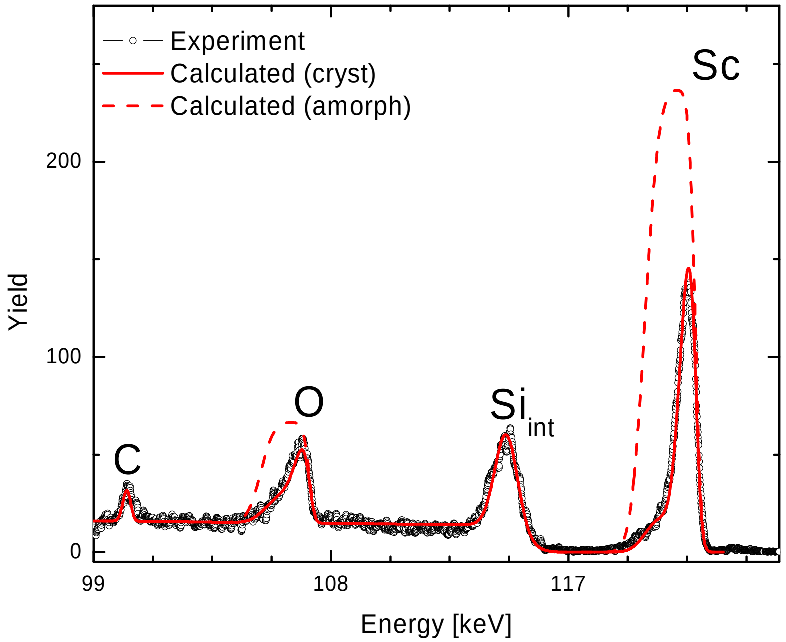

Analysis of film composition was done in a double aligned geometry

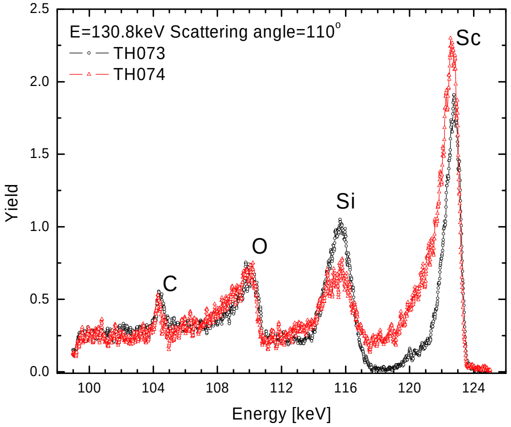

- Surface carbon species concentration is relatively high
- no interface Sc and O are observed = near ideal interface!
- interfacial Si peak intensity and position implies crystalline Si(111) surface
- $\chi = \text{Yield}_{cryst}/\text{Yield}_{amorph} = 4\%$, indicating good film crystalline quality

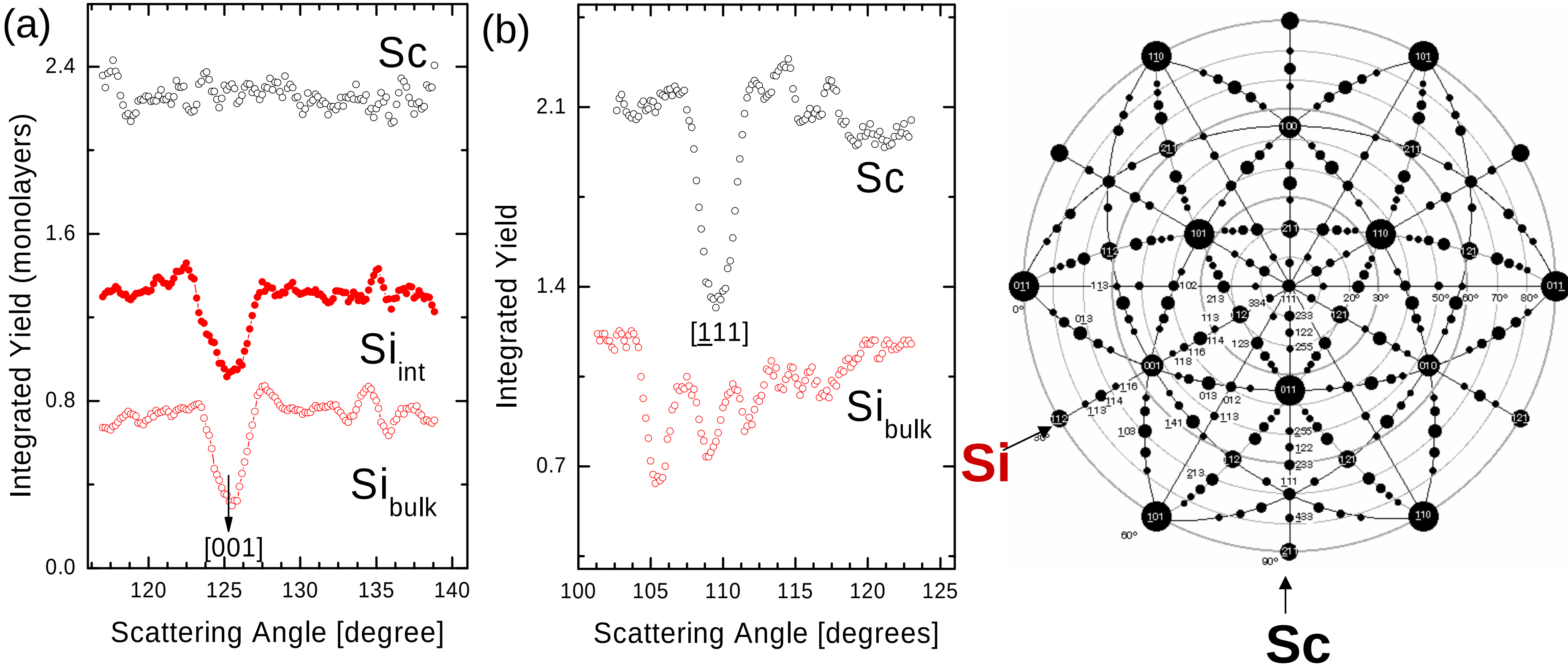

Angular distribution of H^+ions in the Si[$\underline{11}$2] plane. The ions were [111] incident. It shows no evident minima for Sc yields in this geometry, where detector position is aligned with the Si substrate blocking (figure a). However, shifting detector position to a different range of scattering angles (figure b) reveals blocking minima in Sc yields. Position of the Sc blocking minimum can be located according to the stereographic projection of the (111) faced cubic crystal and corresponds to the [$\underline{2}$11] scattering plane.

Sc_2O_3 [111] || Si[111]

Sc_2O_3 [$\underline{2}$11] || Si[$\underline{11}$2] Sc_2O_3 films is rotated azimuthally by 60º with respect to Si

MEIS spectra of low energy dopant implants: ultrashallow junctions

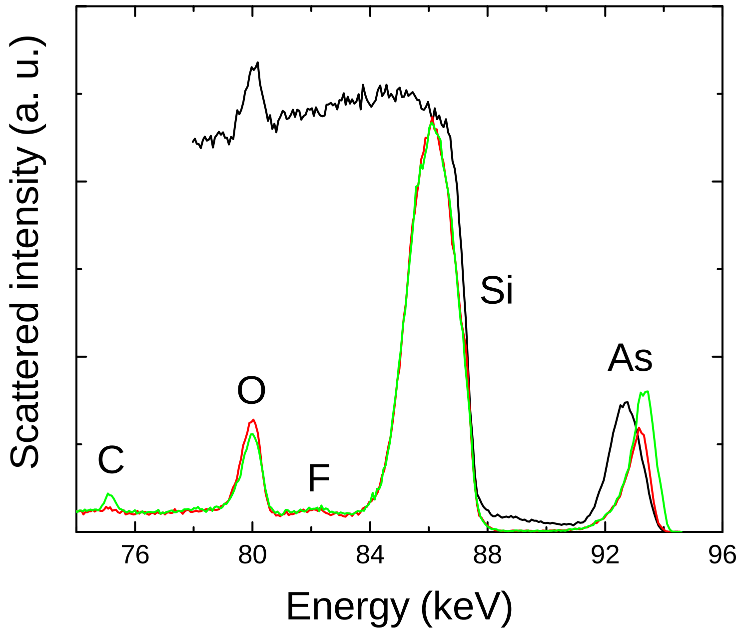

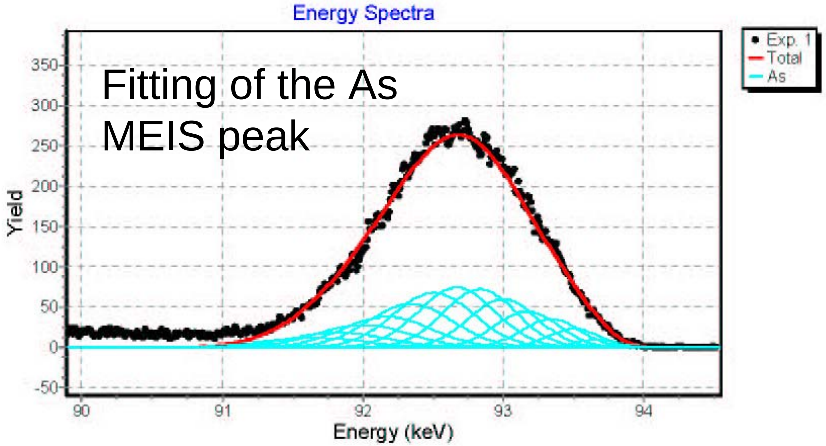

Fitting of the As MEIS peak

Depth profile of As in Si from a low energy implant (1kV, ~10^{15} As/cm^2)

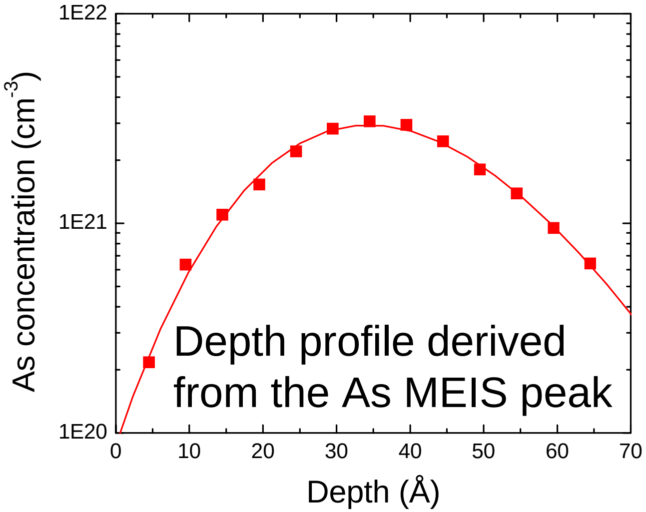

Depth profile derived from the As MEIS peak

Ion Scattering Results

- MEIS useful for compositional profiling and interdiffusion of ultrathin films
- Amorphous high-K films on Si usually compositionally layered with SiO_2 at the interface; native oxides of Ge and GaAs easier to control
- Interface growth on high-K is T-dependent, faster than DG, and self-limiting.
- Mechanism proposed for high-K film decomposition – SiO desorption and silicide formation on Si; GeO from Ge…
- Should include gas-surface adsorption/desorption processes to understand high-T stability – modified SG plot.
- Isotopic labeling studies show rapid exchange and diffusion of gas phase oxygen with film
- Nitride layers help control interdiffusion, interface growth and crystallization
- Important differences between different high-K oxides: absorption of gases (H_2O, CO_2, O_2, H_2) and silicate formation enhanced in La, Gd, Y, and Ce.
- Ion scattering very useful for examining epitaxial overlayers and dopants

Interface electronic structure in multilayer stacks:

Band alignment, “effective” work function, energy gap, permittivity, E_f pinning, charge injection and transport …

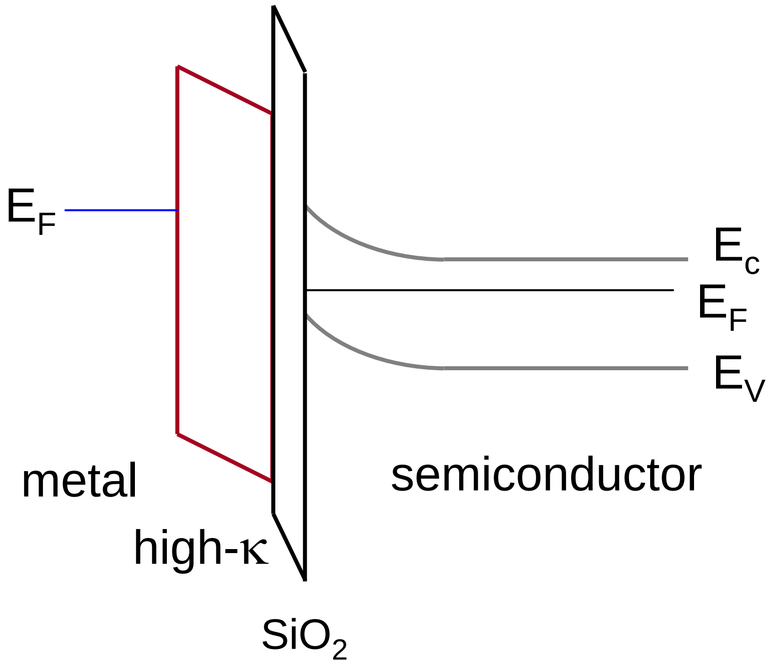

- Band edge energies determined in many ways - optical spectroscopy, electrically (I-V, C-V, V_t, V_{fb}, tunneling) …
- Can we use spectroscopy to (i) measure energies and LDOS more precisely, and (ii) obtain information about interface dipoles and band alignment?

Experimental tools

Photoemission

Inverse photoemission

Internal photoemission

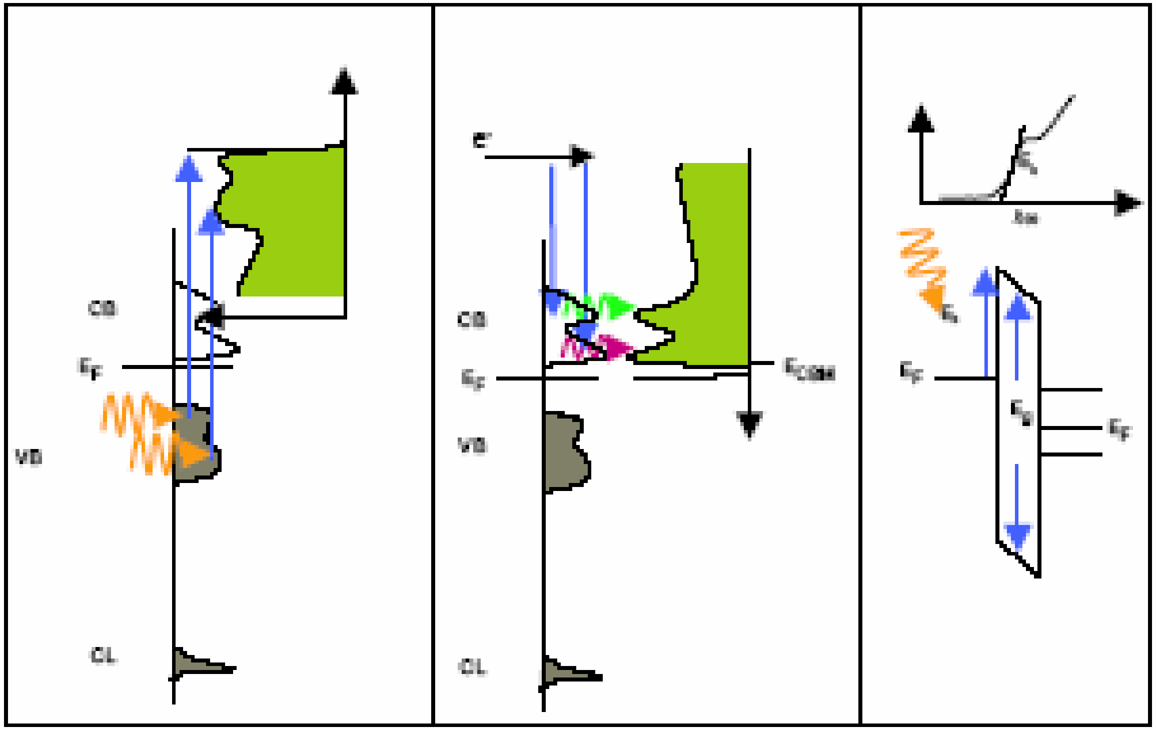

Schematic drawing of three methods to determine band alignment: photoemission, inverse photoemission and internal photoemission. VB = valance band, CB = conduction band, CL = core level

Photoemission and inverse photoemission of high-K gate stack

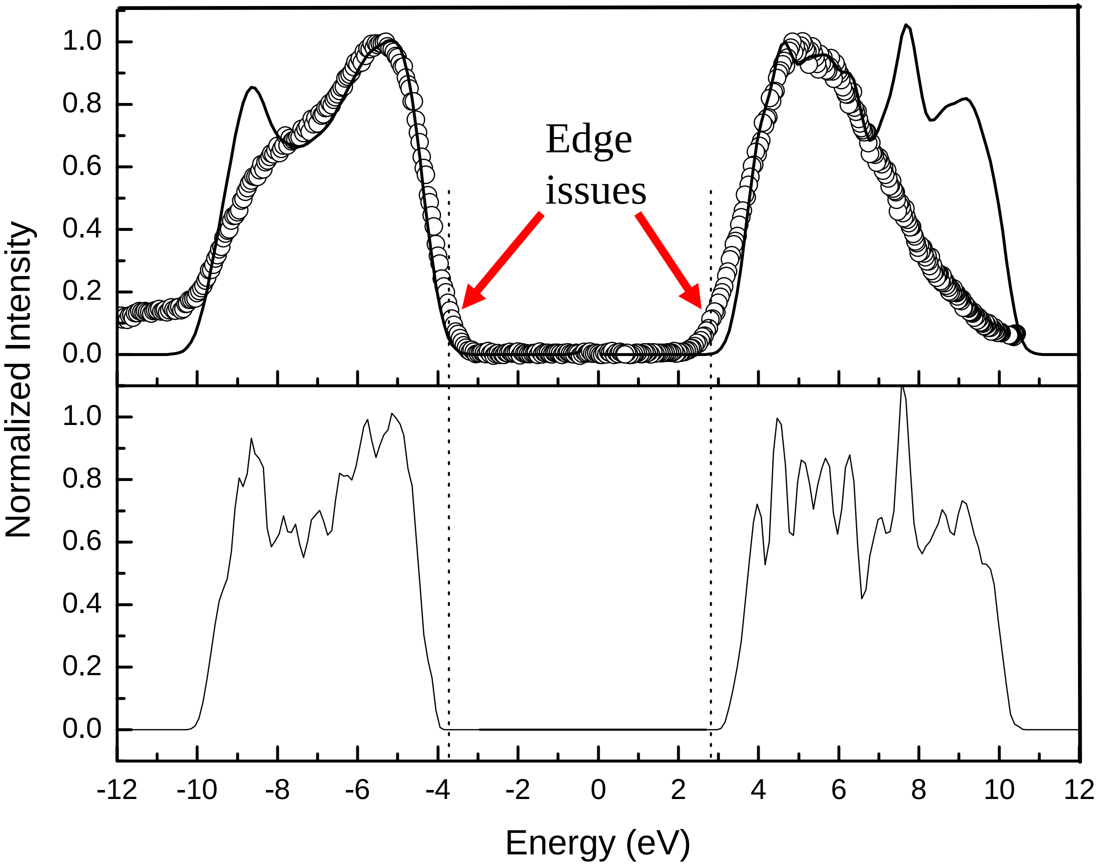

- Experimental results compared with broadened theoretical ones

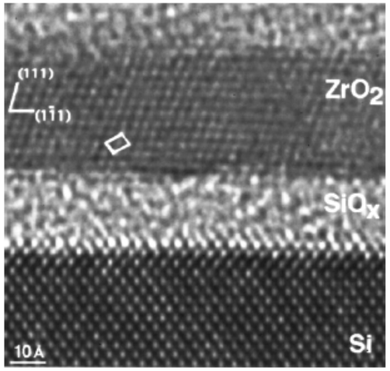

- Check phase with TEM, XRD

- General agreement between theory and experiment is OK (width of bands, main features). Agreement better if corrected for cross-sections.

- However…disagreement between theory and experiment close the band edges for crystalline phases. Band tail states, interface states, defects, multiple phases??? Amorphous phase DOS fits much better.

Effects of alloying and metallization on unoccupied densities of states

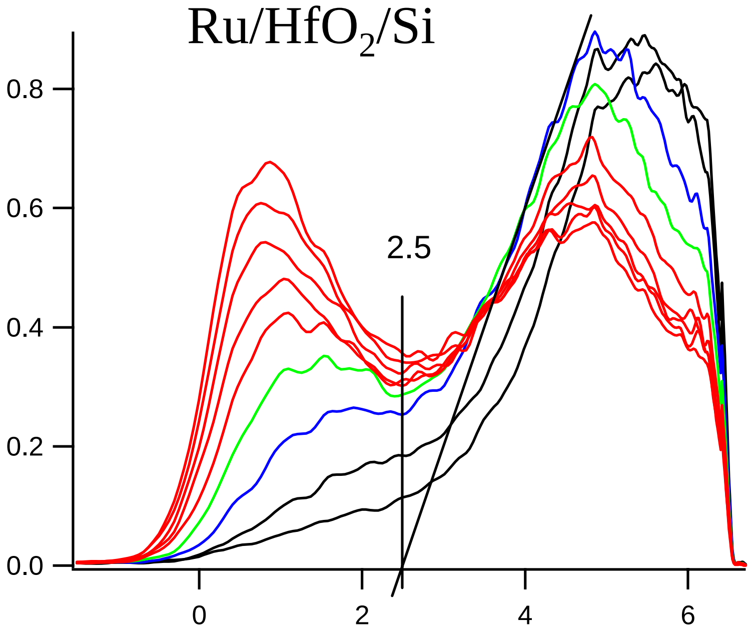

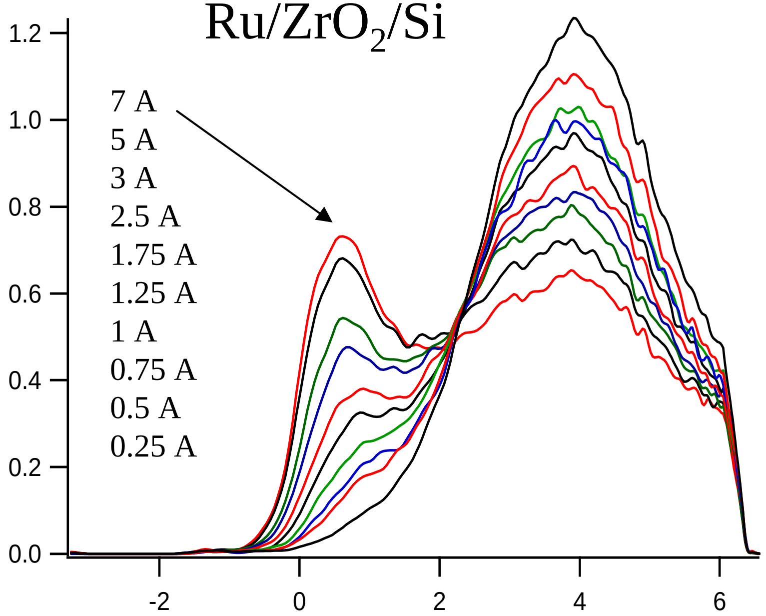

Summary of interface electronic structure

- DOS and permittivity very phase dependent with band tail states
- Work function is not best energy reference for band alignment
- Must develop tools to see and control interface properties – we are working on direct, inverse and internal photoemission
- More generally….atomic composition, structure and bonding at interface are key to understanding system properties in CMOS nano-electronics, especially electrical ones.

ALD growth and film initiation

How does growth start on HF-last?

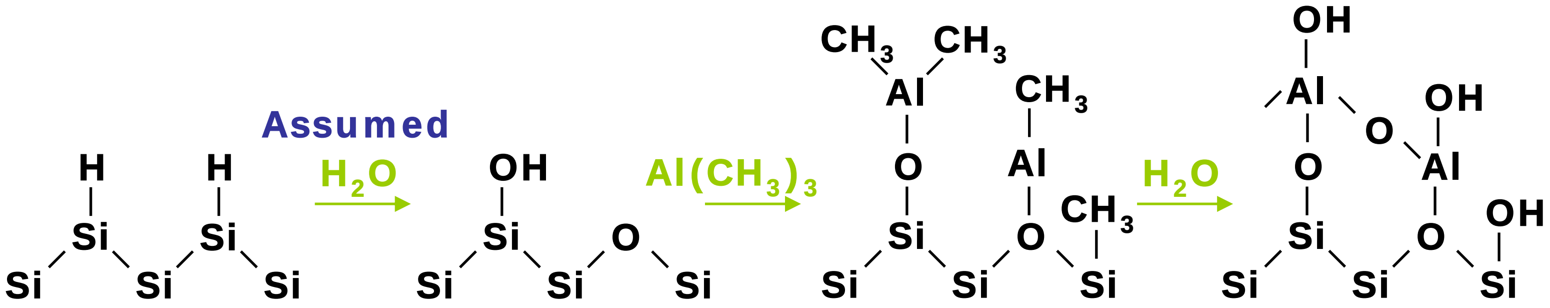

H/Si(111): defect-free

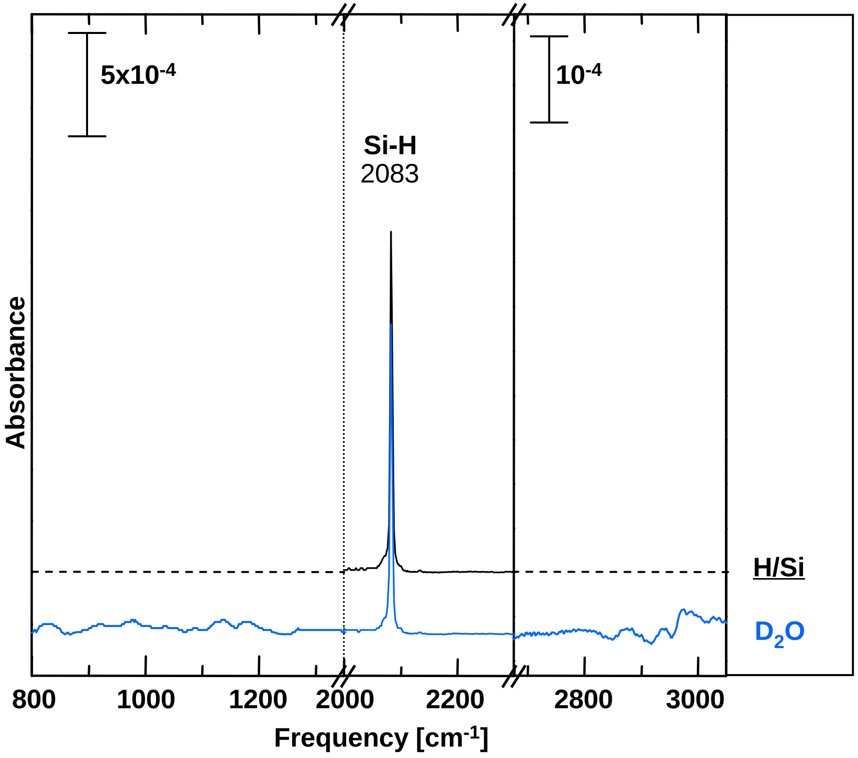

H/Si(100): atomically rough

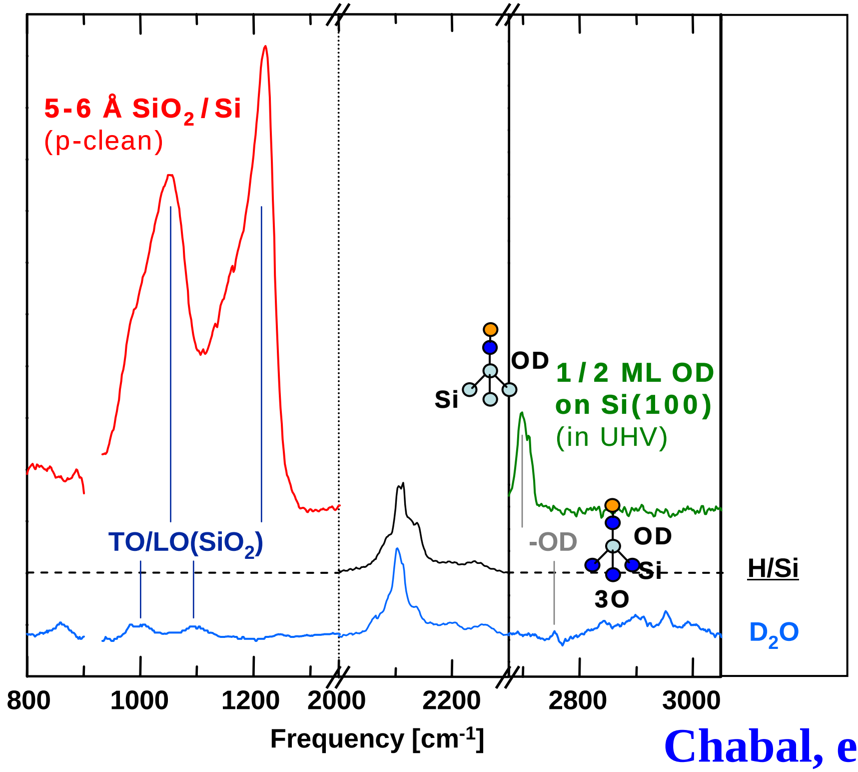

Chabal, et al

Long TMA pulse initiates growth

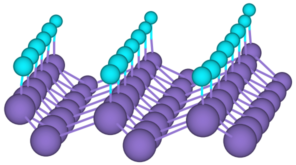

H/Si(111): defect-free

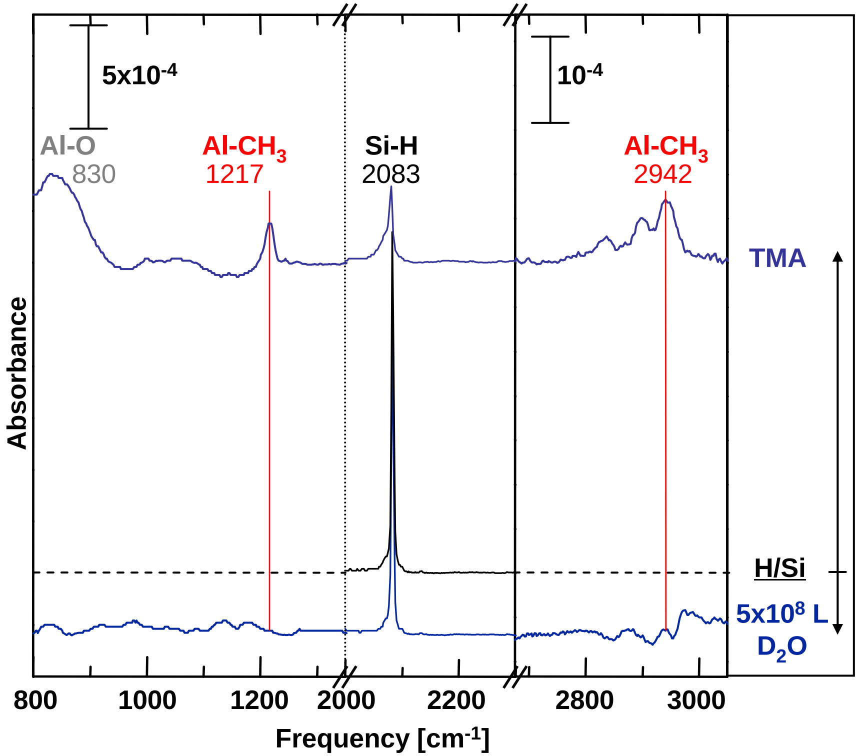

H/Si(100): atomically rough

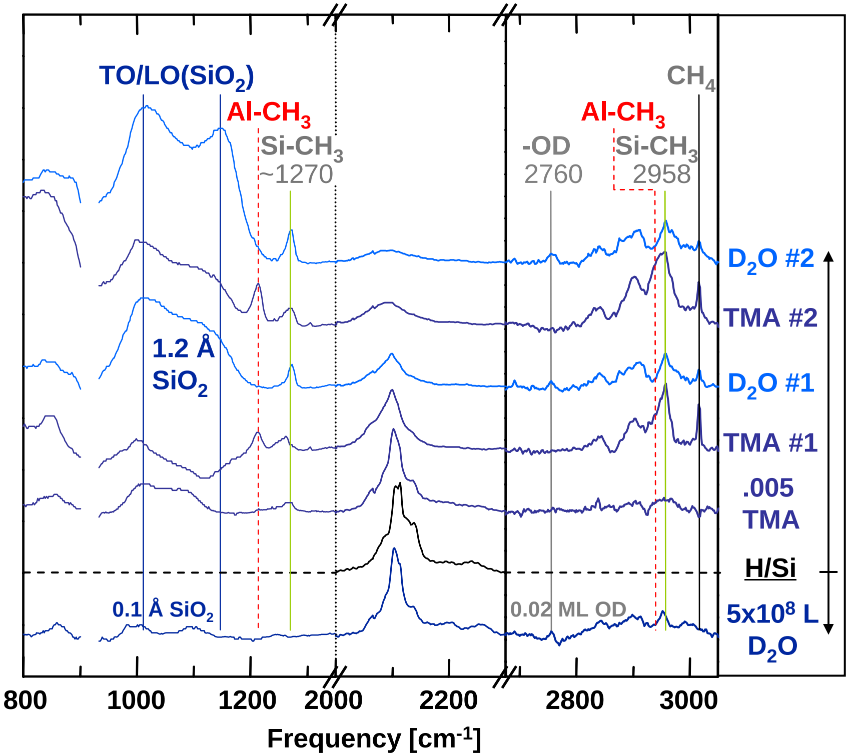

⇒ Not water, but long TMA pulse initiates growth

Chabal, et al

HfO_2 Growth on Pre-functionalized Surfaces

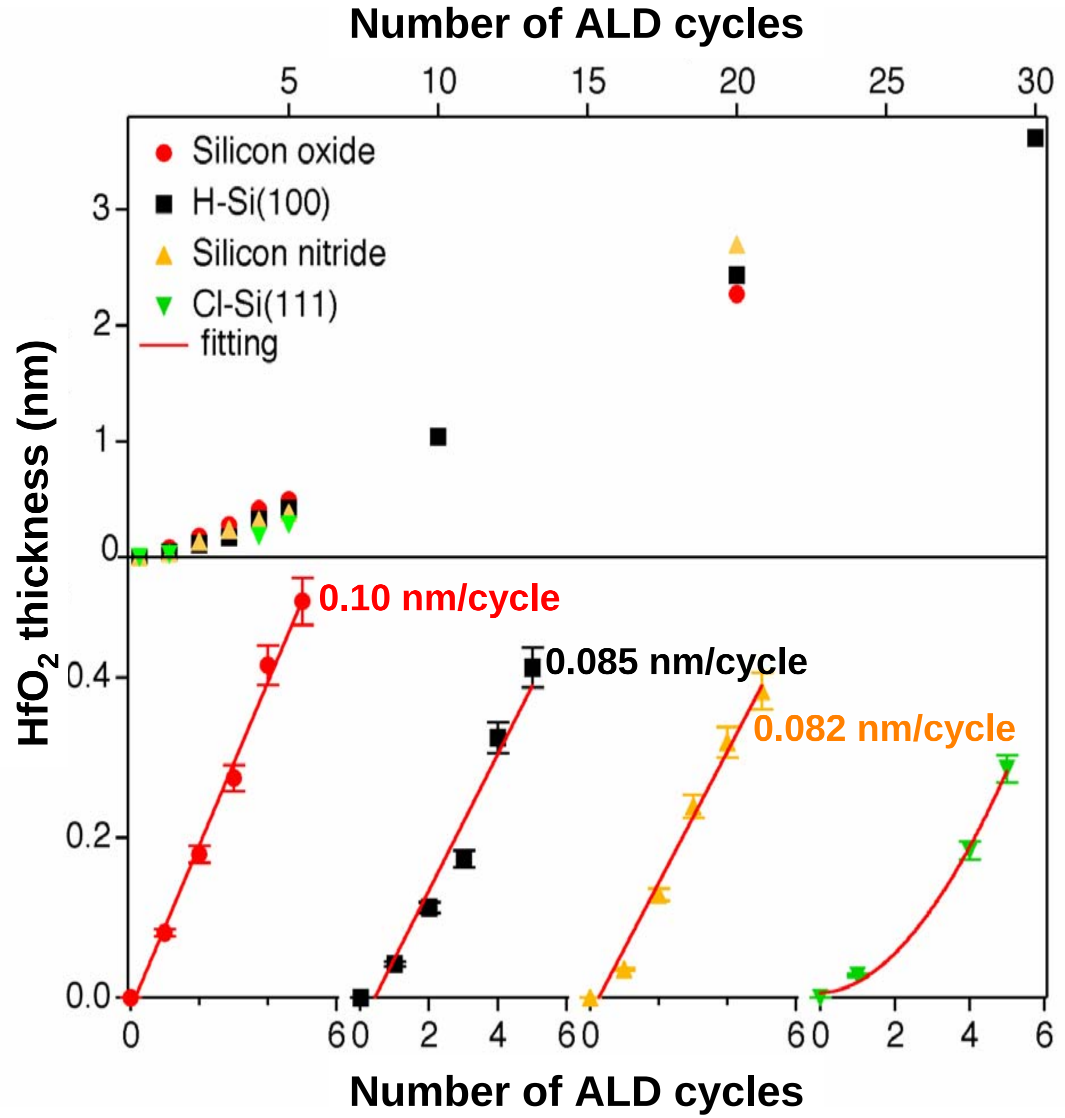

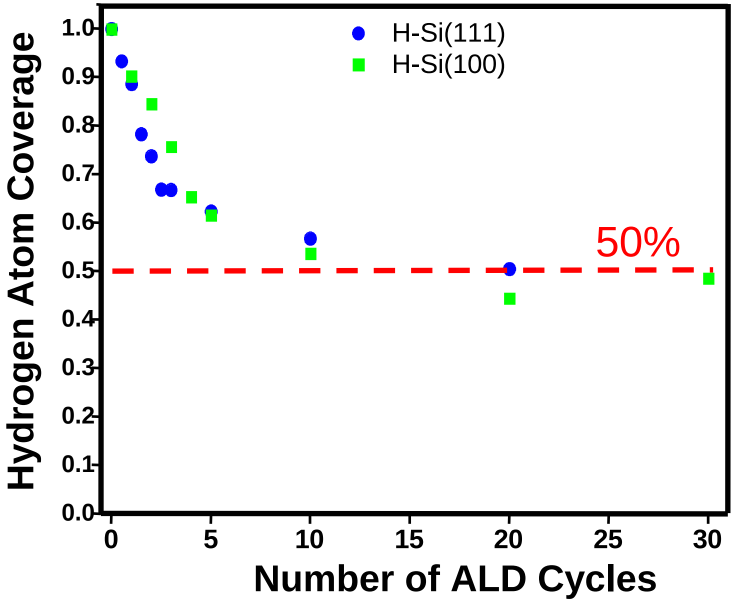

- **Linear growth on SiO_2.**
  Growth rate is ~0.09 nm/cycle
- **No growth barrier on H/Si and Si_xN_y.**
  (*comparable to SiO_2*)
- **Weak Incubation period on Cl/Si**
- **Hydrogen stays on surface w/growth**

Chabal, et al

Rutgers CMOS Front End Research Effort

- Ion scattering – Gustafsson and Garfunkel (FEPTC)
- Photoemission – Bartynski, Madey, Garfunkel
- Inverse photoemission – Bartynski
- Internal photoemission – Garfunkel
- Theory – Vanderbilt
- FTIR - Chabal
- Growth – Chabal, Garfunkel
- Electrical – Cheung…
- XAS, XRD, TEM, SPM…

Rutgers – the State University of New Jersey